AFOSR-TR-97

0290

REPORT DOCUMENTATION PAGE

1. AGENCY USE ONLY (Leave blank)	2. REPORT DATE	3. REPORT TYPE AND DATES COVERED
	15 Aug 96	final 95/02/01 – 96/11/30

4. TITLE AND SUBTITLE
Numerical Simulation of BGK-Burnett Equations

5. FUNDING NUMBERS
F4962C-95-1-0125

6. AUTHOR(S)
Ramesh Agarwal, Ramesh Balakrishnan

7. PERFORMING ORGANIZATION NAME(S) AND ADDRESS(ES)
Wichita St. U.
Wichita KS 67260-0044

8. PERFORMING ORGANIZATION REPORT NUMBER

9. SPONSORING/MONITORING AGENCY NAME(S) AND ADDRESS(ES)
Air Force Office Of Scientific Research
Aerospace & Materials Sciences Directorate
110 Duncan Avenue, Suite B-115
Bolling AFB DC 20332-0001
NA

10. SPONSORING/MONITORING AGENCY REPORT NUMBER

11. SUPPLEMENTARY NOTES

12a. DISTRIBUTION/AVAILABILITY STATEMENT
APPROVED FOR PUBLIC RELEASE
DISTRIBUTION IS UNLIMITED

12b. DISTRIBUTION CODE

In this paper two different forms of Burnett equations are studied which have been designated as 'Augmented Burnett Equations' and 'BGK-Burnett Equations'. The augmented Burnett equations were developed by Zhong to stabilize the solution of the conventional Burnett equations which were derived in 1935 by Burnett from the Boltzmann equation using the second-order Chapman-Enskog expansion. In this formulation, The conventional Burnett equations are augmented by adding *ad hoc* third-order derivatives to stress and heat transfer terms so that the augmented equations are stable to small wavelength disturbances. The BGK-Burnett equations have been recently derived by Agarwal and Balakrishnan from the Boltzmann equation using the Bhatnagar-Gross-Krook (BGK) approximation for the collision integral. These equations have been shown to be entropy consistent and satisfy the Boltzmann H-Theorem in contrast to the conventional Burnett equations which violate the second law of thermodynamics. In this paper, both sets of Burnett equations are applied to compute a 2-D hypersonic flow over a circular cylinder at Knudsen numbers 0.001 to 0.1. The radius of the cylinder, which is the

19970616 120

14. SUBJECT TERMS
Burnett Equations

15. NUMBER OF PAGES

16. PRICE CODE

17. SECURITY CLASSIFICATION OF REPORT	18. SECURITY CLASSIFICATION OF THIS PAGE	19. SECURITY CLASSIFICATION OF ABSTRACT	20. LIMITATION OF ABSTRACT
unclas.	unclas.	unclas	unlim.

NUMERICAL SIMULATION OF BGK-BURNETT EQUATIONS

Project Report

Prepared for

Air Force Office of Scientific Research
Directorate of Aerospace Sciences
AFOSR/NA
Bolling AFB
Washington DC 20332-6448

Principal Investigator
Dr. Ramesh K. Agarwal

Graduate Research Assistant
Ramesh Balakrishnan

Department of Aerospace Engineering
Wichita State University
Wichita, Kansas 67260-0044

August 15, 1996

ABSTRACT

Recently[1] it has been shown using Boltzmann's H-Theorem that the conventional Burnett equations violate the second law of thermodynamics, and hence must not be employed for fluid dynamic simulations. To overcome this difficulty, a new set of equations, designated the BGK-Burnett equations was derived recently by the authors. A second-order distribution function was derived by employing the Chapman-Enskog expansion on the BGK-Boltzmann equation. Moments of the BGK-Boltzmann equation with the collision invariant vector using the second-order distribution function yield the BGK-Burnett equations. It has been shown by the authors[2] that the BGK-Burnett equations are stable to small wavelength disturbances and that they yield results consistent with the second law of thermodynamics. In order to prove that these equations are indeed entropy consistent, it is shown that the second-order distribution function does not violate Boltzmann's H-Theorem. This new set of equations must be used for computing hypersonic flows at moderate Knudsen numbers. The BGK-Burnett equations are employed to compute the hypersonic shock structure. The results of the computations show that under certain flow conditions, the conventional Burnett equations violate the second law of thermodynamics while the BGK-Burnett equations provide entropy consistent results.

INTRODUCTION

In one of the earliest attempts to solve the Burnett equations, Fiscko and Chapman[3] solved the hypersonic shock structure problem by relaxing an initial solution to steady state. They obtained solutions for a variety of Mach numbers and concluded that the Burnett equations do indeed describe the normal shock structure better than the Navier-Stokes equations at high Mach numbers. The equations were however unstable when the grids were made progressively finer. In a subsequent attempt, Zhong[4] showed that the equations could be stabilized by adding a few *ad hoc* super-Burnett terms (linear third order terms, in order to maintain second order accuracy) to the stress and heat transfer terms in the Burnett equations. This set of equations was termed the "Augmented Burnett" equations. The Augmented Burnett equations did not present any stability problems when they were used to compute the flow parameters in the hypersonic shock structure and hypersonic blunt body problems. However attempts at computing the flowfields for blunt body wakes and flat plate boundary layers even with the Augmented Burnett equations have not been entirely successful. It has been conjectured by Chapman et. al[1,5] that this instability may be due to the fact that the Burnett equations violate the second law of thermodynamics at higher Knudsen numbers.

The main objectives of the present work are:

a) To formulate a methodology for deriving and integrating a new set of entropy consistent Burnett equations (designated as BGK-Burnett) that can be extended to higher dimensions.

b) To check if the constitutive relations for the BGK-Burnett stress and heat transfer terms correctly model the flow properties at high Knudsen numbers.

c) To computationally check if the BGK-Burnett equations are stable to small wavelength disturbances.

The second-order distribution function is derived by representing the collision integral in the Bhatnagar-Gross-Krook (BGK) form and considering the first three terms in the Chapman-Enskog expansion. The BGK form of the collision integral assumes that the collision processes are predominantly binary in nature. In deriving the second order distribution function, an as yet unanswered question is the approximation for the material derivatives that appear in the second order terms. In a recent attempt[6], the first and second order distribution functions were obtained iteratively by perturbation analysis of the 1-D BGK-Boltzmann equation. In this analysis the Euler equations were used to approximate the material derivatives in the first order distribution function. Moments of the BGK-Boltzmann equation with the collision invariant vector and the first order distribution function yield the Navier-Stokes equations. In order to keep in step with the iterative process the Navier-Stokes equations were used to approximate the material derivatives in the second order terms. The BGK-Burnett equations are obtained by taking moments of the BGK-Boltzmann equation with the collision invariant vector and the second-order distribution function. This set of equations contains all the stress and heat transfer terms reported by Fiscko and Chapman[3] and has additional terms which are similar to the Super-Burnett terms.

In order to prove analytically that these equations are indeed entropy consistent it has been shown that the second-order distribution function does not violate the H-theorem. Since the definition of the Maxwellian and the higher-order distribution functions used in deriving the BGK-Burnett

equations takes into account the internal energy of the molecules and further does not assume the molecules to be monoatomic, a modified H-function has been formulated to prove the H-theorem. In order to ensure that the entropy gradient remains positive throughout the flow field, a set of boundary conditions has been derived using the Gibbs entropy equation. It has been shown that a positive entropy production can be ensured by setting the heat transfer terms to zero at stations far upstream and far downstream of the shock.

1-D BGK-BOLTZMANN EQUATION

The 1-D Boltzmann equation can be written as follows, using the BGK approximation for the collision integral J(f,f).

$$\frac{\partial f}{\partial t} + v\frac{\partial f}{\partial x} = J(f,f) = \nu\left(f^{(0)} - f\right) \qquad (1)$$

In the above equation, f denotes the distribution function, v denotes the molecular velocity, J(f,f) denotes the collision integral, and ν denotes the collision frequency. In this representation the non-linear collision integral is approximated by a single relaxation time model. This approximation assumes that any non-equilibrium distribution function will settle down to the equilibrium distribution exponentially.

ZEROTH-ORDER (MAXWELLIAN) DISTRIBUTION FUNCTION

For the special case of collision equilibrium, the distribution function takes the form shown in eq. (2). It can been shown that this is both a necessary and sufficient condition for collision equilibrium.

$$f = f^{(0)} = \frac{\rho}{I_0}\left(\frac{\beta}{\pi}\right)^{\frac{D_f}{2}} \exp\left[-\beta(v-u)^2 - \frac{I}{I_0}\right] \qquad (2)$$

D_f denotes the number of translational degrees of freedom, u denotes the fluid velocity and $\beta = \frac{1}{2RT}$. I denotes the internal energy that accounts for the energy contribution due to all the non-translational degrees of freedom and I_0 denotes the average internal energy, and is given by the expression

$$I_0 = \frac{(2 + D_f) - \gamma D_f}{2(\gamma - 1)} RT \qquad (3)$$

HIGHER-ORDER DISTRIBUTION FUNCTIONS

The various higher-order distribution functions are obtained by representing them as a Chapman-Enskog asymptotic series expansion.

$$f = f^{(0)} + \xi f^{(1)} + \xi^2 f^{(2)} + \ldots\ldots + \xi^n f^{(n)} + \ldots\ldots\ldots\ldots \qquad (4)$$

where, $\xi = \left(\frac{\lambda}{L}\right)$ denotes the Knudsen number. The first two terms of the Chapman-Enskog expansion give rise to the first-order distribution function $f = f^{(0)} + \xi f^{(1)}$, and the first three terms of the Chapman-Enskog expansion give rise to the second-order distribution function, $f = f^{(0)} + \xi f^{(1)} + \xi^2 f^{(2)}$. In order to obtain exact analytical expressions for the first and second-order distribution functions the BGK-Boltzmann equation is non-dimensionalized by defining the following non-dimensional variables

$$\hat{x}=\frac{x}{L},\ \hat{v}=\frac{v}{C_{rms}},\ \hat{t}=\frac{tC_{rms}}{L},\ \hat{\nu}=\frac{\nu\lambda_{\infty}}{C_{rms}} \tag{5}$$

where, L denotes the characteristic length, C_{rms} denotes the root mean square molecular velocity and λ_{∞} denotes the free stream mean free path. On substituting the non-dimensional variables, eq. (1) takes the following form:

$$\xi\left[\frac{\partial f}{\partial \hat{t}}+\hat{v}\frac{\partial f}{\partial \hat{x}}\right]=\hat{\nu}\left(f^{(0)}-f\right) \tag{6}$$

THE FIRST-ORDER DISTRIBUTION FUNCTION

Substituting the first two terms of the Chapman-Enskog expansion, $f = f^{(0)} + \xi f^{(1)}$, in the BGK-Boltzmann equation and equating like powers of the Knudsen number yields:

$$f^{(1)}=-\frac{1}{\xi\nu}\left[\frac{\partial}{\partial t}\left(f^{(0)}\right)+v\frac{\partial}{\partial x}\left(f^{(0)}\right)\right] \tag{7}$$

On expressing $f^{(1)} = f^{(0)}\Phi^{(1)}$ and substituting in eq. (7) the following expression is obtained. In this expression the 1-D Euler equations have been used to express the time derivatives in terms of the spatial derivatives.

$$\Phi^{(1)}=-\frac{1}{\xi\nu}A^{(1)}(I,c)\frac{\partial\beta}{\partial x}-\frac{1}{\xi\nu}A^{(2)}(I,c)\frac{\partial u}{\partial x} \tag{8}$$

where,

$$A^{(1)}(I,c)=\left[\frac{5c}{2\beta}-\frac{4Ic(\gamma-1)}{(3-\gamma)}-c^{3}\right] \tag{9}$$

$$A^{(2)}(I,c)=\left[\beta c^{2}(3-\gamma)+\frac{(3\gamma-5)}{2}-4I\beta\frac{(\gamma-1)^{2}}{(3-\gamma)}\right] \tag{10}$$

and c denotes the peculiar or thermal velocity, c=v-u. The first-order distribution function satisfies the property $\langle \Psi, f \rangle = \left\langle \Psi, f^{(0)} \right\rangle$. Hence $\left\langle \Psi, \xi f^{(1)} \right\rangle = 0$.

SECOND-ORDER DISTRIBUTION FUNCTION

The second-order distribution function is obtained by considering the first three terms in the asymptotic Chapman-Enskog expansion for the distribution function. Substituting the expression for the second order distribution function in the non-dimensional 1-D BGK-Boltzmann equation and equating like powers of ξ yields:

$$\frac{\partial}{\partial \hat{t}}\left(f^{(1)}\right) + \hat{v}\frac{\partial}{\partial \hat{x}}\left(f^{(1)}\right) = -\hat{v}f^{(2)} \tag{11}$$

From the above equation the following equation for $f^{(2)}$ is obtained:

$$f^{(2)} = -\left(\frac{1}{\xi \nu}\right)\left[\frac{\partial}{\partial t}\left(f^{(1)}\right) + v\frac{\partial}{\partial x}\left(f^{(1)}\right)\right] \tag{12}$$

Since the field vector **Q** is the same, for the Euler , Navier-Stokes and BGK-Burnett equations, moments of the distribution function with the collision invariant vector Ψ must be the same for any distribution function. Hence, the second-order distribution function *must* satisfy the property $\langle \Psi, f \rangle = \left\langle \Psi, f^{(0)} \right\rangle$. This condition translates to the following equation:

$$\left\langle \Psi, \xi^2 f^{(2)} \right\rangle = \left\langle \Psi, -\frac{\xi}{\nu}\left[\frac{\partial}{\partial t}\left(f^{(0)}\Phi^{(1)}\right) + v\frac{\partial}{\partial x}\left(f^{(0)}\Phi^{(1)}\right)\right]\right\rangle = 0 \tag{13}$$

An expression for the second-order distribution function satisfyng the above equation is given by:

$$f = f^{(0)} + \xi f^{(0)}\Phi^{(1)} - \frac{\xi}{\nu}\left[\frac{\partial}{\partial t}\left(f^{(0)}\Phi^{(1)}\right) + \frac{\partial}{\partial x}\left(uf^{(0)}\Phi^{(1)}\right) + \frac{\partial}{\partial x}\left(cf^{(0)}\tilde{\Phi}^{(1)}\right)\right] \tag{14}$$

where,

$$\tilde{\Phi}^{(1)} = -\frac{1}{\xi\nu}\tilde{A}^{(1)}\left(\tilde{I},c\right)\frac{\partial\beta}{\partial x} - \frac{1}{\xi\nu}\tilde{A}^{(2)}\left(\tilde{I},c\right)\frac{\partial u}{\partial x} \tag{15}$$

$$\tilde{A}^{(1)}\left(\tilde{I},c\right) = \left[\frac{\theta_1}{\beta}c + \frac{\theta_2}{\beta}\tilde{I}c + \theta_3 c^3\right] \tag{16}$$

$$\tilde{A}^{(2)}\left(\tilde{I},c\right) = \left[\beta\theta_4 c^2 + \theta_5\tilde{I} + \theta_6\right] \tag{17}$$

In the above expressions $\tilde{I} = \frac{I}{I_0}$ and c denotes the peculiar or thermal velocity, c = v-u. The coefficients θ_i, i = 1,2....6 are functions of the specific heat ratio γ. The exact expressions for these coefficients are given in the appendix.

THE BGK-BURNETT EQUATIONS

The various fluid dynamics equations are obtained by taking moments of the BGK-Boltzmann equation with the collision invariant vector

$$\Psi = \left[1,\ v,\ \left(I + \frac{v^2}{2}\right)\right]^T \tag{18}$$

The moment of f is defined as $\langle\Psi, f\rangle = \int_0^\infty\int_{-\infty}^{\infty}\Psi f\, dv\, dI$. On taking moments of the BGK-Boltzmann equation, the following generic equation is obtained.

$$\frac{\partial}{\partial t}\langle\Psi, f\rangle + \frac{\partial}{\partial x}\langle\Psi, vf\rangle = \left\langle\Psi, \nu\left(f^{(0)} - f\right)\right\rangle = 0 \tag{19}$$

On substituting the zeroth, first and second-order distribution functions the Euler, Navier-Stokes and BGK-Burnett equations are obtained respectively.

$$\frac{\partial}{\partial t}\left[\int_0^{\infty}\int_{-\infty}^{\infty} f\Psi \, dvdI\right]+\frac{\partial}{\partial x}\left[\int_0^{\infty}\int_{-\infty}^{\infty} vf\Psi \, dvdI\right]=\nu\int_0^{\infty}\int_{-\infty}^{\infty}\Psi\left(f^0-f\right)dvdI=0 \tag{20}$$

Moments of the BGK-Boltzmann equation with Ψ using the second-order distribution function yield the BGK-Burnett Equations.

$$\frac{\partial}{\partial t}\left\langle \Psi, f^{(0)}+\xi f^{(1)}+\xi^2 f^{(2)}\right\rangle+\frac{\partial}{\partial x}\left\langle \Psi, v\left(f^{(0)}+\xi f^{(1)}+\xi^2 f^{(2)}\right)\right\rangle=\left\langle \Psi, v\left(f^{(0)}-f\right)\right\rangle \tag{21}$$

The 1-D BGK-Burnett equations are represented in conservation law form as:

$$\frac{\partial Q}{\partial t}+\frac{\partial G^i}{\partial x}+\frac{\partial G^v}{\partial x}+\frac{\partial G^B}{\partial x}=0 \tag{22}$$

The elements of the field and flux vectors are:

$$Q=\begin{bmatrix}\rho\\ \rho u\\ \rho e\end{bmatrix},\ G^i=\begin{bmatrix}\rho u\\ p+\rho u^2\\ pu+\rho ue\end{bmatrix},\ G^v=\begin{bmatrix}0\\ -\tau_x^{N-S}\\ -u\tau_x^{N-S}+q^{N-S}\end{bmatrix}\ \text{and}\ G^B=\begin{bmatrix}0\\ -\tau_x^{B}\\ -u\tau_x^{B}+q^{B}\end{bmatrix} \tag{23}$$

The Navier-Stokes and BGK-Burnett stress and heat transfer terms are given by the following expressions.

$$\tau_x^{N-S}=\frac{4}{3}\mu\frac{\partial u}{\partial x},\ \text{and}\ q^{N-S}=-k\frac{\partial T}{\partial x} \tag{24}$$

$$\tau_x^{B}=-\frac{\mu^2}{p}\left[\begin{array}{l}a^{(1)}\left(\frac{\partial u}{\partial x}\right)^2+a^{(2)}\frac{T}{\rho}\left(\frac{\partial^2\rho}{\partial x^2}\right)+a^{(3)}\frac{T}{\rho^2}\left(\frac{\partial\rho}{\partial x}\right)^2+a^{(4)}\frac{1}{\rho}\left(\frac{\partial\rho}{\partial x}\right)\left(\frac{\partial T}{\partial x}\right)\\ +a^{(5)}\frac{1}{T}\left(\frac{\partial T}{\partial x}\right)^2+a^{(6)}\left(\frac{\partial^2 T}{\partial x^2}\right)\end{array}\right] \tag{25}$$

$$-\frac{\mu^3}{p^2}\left[a^{(7)}\frac{T}{\rho}\left(\frac{\partial\rho}{\partial x}\right)\left(\frac{\partial^2 u}{\partial x^2}\right)+a^{(8)}\frac{1}{Pr}\left(\frac{\partial u}{\partial x}\right)\left(\frac{\partial^2 T}{\partial x^2}\right)+a^{(9)}T\left(\frac{\partial^3 u}{\partial x^3}\right)+a^{(10)}\left(\frac{\partial u}{\partial x}\right)^3\right]$$

$$q_x^B = \frac{\mu^2}{\rho}\left[b^{(1)}\frac{1}{T}\left(\frac{\partial u}{\partial x}\right)\left(\frac{\partial T}{\partial x}\right) + b^{(2)}\left(\frac{\partial^2 u}{\partial x^2}\right) + b^{(3)}\frac{1}{\rho}\left(\frac{\partial \rho}{\partial x}\right)\left(\frac{\partial u}{\partial x}\right)\right]$$
$$+\frac{\mu^3}{p\rho}\left[\begin{array}{l} b^{(4)}\left(\frac{\partial u}{\partial x}\right)\left(\frac{\partial^2 u}{\partial x^2}\right) + b^{(5)}\frac{1}{TPr}\left(\frac{\partial T}{\partial x}\right)\left(\frac{\partial^2 T}{\partial x^2}\right) + b^{(6)}\frac{1}{\rho Pr}\left(\frac{\partial \rho}{\partial x}\right)\left(\frac{\partial^2 T}{\partial x^2}\right) \\ +b^{(7)}\frac{1}{Pr}\left(\frac{\partial^3 T}{\partial x^3}\right) + b^{(8)}\frac{1}{T}\left(\frac{\partial T}{\partial x}\right)\left(\frac{\partial u}{\partial x}\right)^2 + b^{(9)}\frac{1}{\rho}\left(\frac{\partial \rho}{\partial x}\right)\left(\frac{\partial u}{\partial x}\right)^2 \\ +b^{(10)}\frac{1}{T^2 Pr}\left(\frac{\partial T}{\partial x}\right)^3 \end{array}\right] \qquad (26)$$

The coefficients $a^{(1)}$ - $a^{(10)}$ and $b^{(1)}$ - $b^{(10)}$ in the expressions for the BGK-Burnett stress and heat transfer terms are functions of 'γ' and are given in the appendix. The BGK-Burnett stress and heat transfer terms have two sets of terms of orders μ^2 and μ^3. The former results when the Euler equations are used to express the material derivatives in terms of the spatial derivatives and the latter is obtained when the Navier-Stokes equations are used to express the material derivatives in terms of the spatial derivatives. When only terms of order μ^2 are considered it is observed that the derivatives in the expressions for the stress and heat transfer terms are identical to the derivatives reported by Fiscko and Chapman[3]. The coefficients of these derivatives are, however, very different to those in Ref. 3. Table 1. shows the comparison between the BGK-Burnett coefficients and the coefficients of the Burnett equations in Ref. 3. When terms up to the order μ^3 are considered it is observed that there are many non-linear terms (products of derivatives) in addition to linear third-order derivatives. These derivatives are similar to the super-Burnett derivatives in Ref. 3. Table 2. and Table. 3. show the comparisons between the coefficients of the BGK-Burnett derivatives and the coefficients of the augmented Burnett terms evaluated by Zhong[4].

LINEARIZED STABILITY ANALYSIS

It has been shown by Bobylev[7] that the conventional Burnett equations are not stable to small wavelength disturbances. Hence the conventional Burnett equations tend to blow up when the mesh sizes are made progressively finer. In order to investigate the stability aspects of the BGK-Burnett equations a model problem is considered which studies the response of a uniform gas to a 1-D periodic perturbation wave. The initial density, temperature and velocity of the undisturbed gas at time t = 0 are ρ_0, T_0, and $u_0 = 0$ respectively. At t = 0 the gas is perturbed such that:

$$\rho = \rho_0\left(1 + C_1 e^{\frac{i\omega x}{L_0}}\right) \tag{27}$$

$$T = T_0\left(1 + C_2 e^{\frac{i\omega x}{L_0}}\right) \tag{28}$$

$$u = \sqrt{RT_0}\left(C_3 e^{\frac{i\omega x}{L_0}}\right) \tag{29}$$

Since the perturbations are assumed to be small the magnitudes of the coefficients in the expressions (27)-(29) are required to satisfy the inequality $|C_k| << 1$, $(k = 1,2,3)$.

The characteristic length $L_0 = \dfrac{\mu_0}{\rho_0\sqrt{RT_0}} = 0.783\lambda$, where λ denotes the mean free path. The non-dimensional circular frequency $\omega = \dfrac{2\pi}{\left(L/L_0\right)} = 4.92\dfrac{\lambda}{L} = 4.92Kn$. Introducing the perturbed quantities in the continuity, momentum and energy equations and simplifying yields:

$$\frac{\partial V'}{\partial t'} + M_1 \frac{\partial V'}{\partial x'} + M_2 \frac{\partial^2 V'}{\partial x'^2} + M_3 \frac{\partial^3 V'}{\partial x'^3} + M_4 \frac{\partial^4 V'}{\partial x'^4} = 0 \qquad (30)$$

$$V' = \begin{Bmatrix} \rho' \\ u' \\ T' \end{Bmatrix}, \; M_1 = \begin{bmatrix} 0 & 1 & 0 \\ 1 & 0 & 1 \\ 0 & (\gamma - 1) & 0 \end{bmatrix}, \; M_2 = \begin{bmatrix} 0 & 0 & 0 \\ 0 & -(3-\gamma) & 0 \\ 0 & 0 & \frac{\gamma}{Pr} \end{bmatrix}, \; M_3 = \begin{bmatrix} 0 & 0 & 0 \\ \frac{a^{(2)}}{R} & 0 & \frac{a^{(6)}}{R} \\ 0 & b^{(2)}(\gamma - 1) & 0 \end{bmatrix},$$

$$M_4 = \begin{bmatrix} 0 & 0 & 0 \\ 0 & \frac{a^{(9)}}{R} & 0 \\ 0 & 0 & \frac{b^{(7)}(\gamma - 1)}{R\,Pr} \end{bmatrix}.$$

The non-dimensional initial conditions for eq. (30) can be denoted in vector form as $V'|_{t=0} = \overline{V} e^{i\omega x'}$, where $x' = \frac{x}{L_0}$. Let us assume the solution of the above equation to be of the form

$$V' = \overline{V} e^{i\omega x'} e^{\phi t'} \qquad (31).$$

where, $t' = \frac{t p_0}{\mu_0}$. The complex variable $\phi = \alpha + i\beta$. α denotes the attenuation coefficient and β denotes the dispersion coefficient. For stability $\alpha < 0$ as L decreases or in other words the flow must attenuate as the Knudsen number increases. Substituting eq. (31) in eq. (30) and simplifying yields eq. (32) when Euler equations are used to express the material derivatives.

$$\left[\Phi I + i\omega M_1 - \omega^2 M_2 - i\omega^3 M_3\right] V_0 e^{i\omega x'} e^{\Phi t'} = 0 \qquad (32)$$

For a non-trivial solution the following condition must be satisfied

$$\left|\Phi I + i\omega M_1 - \omega^2 M_2 - i\omega^3 M_3\right| = 0 \qquad (33)$$

When the Navier-Stokes equations are used to express the material derivatives in terms of the spatial derivatives the following equation is obtained:

$$\left[\Phi I + i\omega M_1 - \omega^2 M_2 - i\omega^3 M_3 + \omega^4 M_4\right] V_0 e^{i\omega x'} e^{\Phi t'} = 0 \tag{34}$$

For non-trivial solutions the following condition must be satisfied:

$$\left|\Phi I + i\omega M_1 - \omega^2 M_2 - i\omega^3 M_3 + \omega^4 M_4\right| = 0 \tag{35}$$

The trajectory of the roots of the characteristic equations (33) and (35) is plotted on the complex plane on which the real axis denotes the attenuation coefficient and the imaginary axis denotes the dispersion coefficient. For stability it is required that the roots lie to the left of the imaginary axis as the Knudsen number increases. Fig(s) 1-4 show the trajectory of the roots of the characteristic equation as the Knudsen number increases. From the plots it is observed that unconditional stability is guaranteed only when the Navier-Stokes equations are used to express the material derivatives in terms of the spatial derivatives. It must be noted, however, that the linear stability analysis does not consider the many non-linear terms - powers and products of derivatives - that are present in the BGK-Burnett stress and heat transfer terms. Hence, this analysis, is at best only a necessary condition for the stability of these equations. A more rigorous proof of the stability of these equations involves verifying the Boltzmann's H-Theorem.

BOLTZMANN'S H-THEOREM

The BGK-Burnett equations must satisfy the second-law of thermodynamics. There, however, is no acceptable definition of entropy for a gas in a state of non-equilibrium. Physical intuition tells us that an isolated system will evolve from an arbitrary initial state to a state of equilibrium.

Boltzmann's H theorem formalizes this notion, and also makes explicit the manner in which this evolution proceeds. A spatially homogenous gas is defined as one in which the density does not vary with position. Boltzmann's H theorem states that for a spatially homogenous gas the inequality, $\frac{\partial}{\partial t}(H) \le 0$, must be satisfied when the gas approaches equilibrium. The quantity H which is shown to be the kinetic theory equivalent of entropy[1] is defined as $H = \int_{-\infty}^{\infty} f \ln f \, dv$. In arriving at this definition of the H-function Boltzmann made the following assumptions:

a) The molecules comprising the gas do not have any internal energy. Hence the H function was defined *only* over the range of molecular velocities.

b) The gas was assumed to be monoatomic.

Since our definition of the Maxwellian and the first and second order distribution functions takes into account the energy contribution due to the various non-translational degrees of freedom and further does not assume the gas to be monoatomic, the definition of H must be modified to account for these differences. The modified definition of the H function can be shown to reduce to the classical (Boltzmann) definition of H for the specific case of a monoatomic gas.

MODIFIED H-FUNCTION

The change in entropy in classical thermodynamics is given by the following expression:

$$(s_2 - s_1) = C_v \ln \frac{T_2}{T_1} - R \ln \frac{\rho_2}{\rho_1} \qquad (36)$$

[1] It must be noted that entropy according to classical thermodynamics is defined *only* for equilibrium systems. The quantity 'H' , however, is defined *even* for non-equilibrium systems.

where the subscripts '1' and '2' denote thermodynamic variables at equilibrium stations far upstream and far downstream respectively. The absolute entropy is given by the following expression up to an additive constant.

$$s = C_v \ln T - R \ln \rho + R\mathcal{C}_0 \tag{37}$$

The above expression can be cast in the form

$$s = -R\left[\ln \rho + \frac{\ln \beta}{(\gamma - 1)} - \mathcal{C}_0\right] \tag{38}$$

where $\beta = \frac{1}{2RT}$. We now need to devise a method to arrive at the above expression from the Maxwellian distribution function which is also the equilibrium distribution function. The 1-D Maxwellian distribution function is given by the expression

$$f^{(0)} = F = \frac{\rho}{I_0}\sqrt{\frac{\beta}{\pi}} \exp\left[-\frac{I}{I_0} - \beta(v-u)^2\right] \tag{39}$$

where the average internal energy $I_0 = \frac{(3-\gamma)}{4\beta(\gamma-1)}$. Equation (40) can be rewritten as:

$$\begin{aligned} \ln f^{(0)} = \ln F = &\left[\ln \rho + \frac{3}{2}\ln \beta + \ln\left\{\frac{4(\gamma-1)}{(3-\gamma)\sqrt{\pi}}\right\} - \beta u^2\right] \\ &- \frac{4\beta(\gamma-1)}{(3-\gamma)} I - 2\beta\left(\frac{v^2}{2}\right) + (2\beta u)v \end{aligned} \tag{41}$$

On rearranging the terms in eq. (41)

$$\begin{aligned} \ln f^{(0)} - 2\beta I\frac{(5-3\gamma)}{(3-\gamma)} = &\left[\ln \rho + \frac{3}{2}\ln \beta + \ln\left\{\frac{4(\gamma-1)}{(3-\gamma)\sqrt{\pi}}\right\} - \beta u^2\right] \\ &- 2\beta\left(I + \frac{v^2}{2}\right) + (2\beta u)v \end{aligned} \tag{42}$$

Equation (42) is indeed a linear combination[2] of the collision invariants. Hence,

$$\left\langle \left\{ \ln f^{(0)} - 2\beta I \frac{(5-3\gamma)}{(3-\gamma)} \right\} \left(\frac{\partial f^{(0)}}{\partial t} + v \frac{\partial f^{(0)}}{\partial x} \right) \right\rangle = \int_0^\infty \int_{-\infty}^\infty \left\{ \ln f^{(0)} - 2\beta I \frac{(5-3\gamma)}{(3-\gamma)} \right\} \left(\frac{\partial f^{(0)}}{\partial t} + v \frac{\partial f^{(0)}}{\partial x} \right) dv\, dI = 0 \tag{43}$$

The above equation can be recast in the following form by making use of the identity

$$\left\langle \left(\frac{\partial f^{(0)}}{\partial t} + v \frac{\partial f^{(0)}}{\partial x} \right) \right\rangle = 0.$$

$$\left\langle \left\{ 1 + \ln f^{(0)} - 2\beta I \frac{(5-3\gamma)}{(3-\gamma)} \right\} \left(\frac{\partial f^{(0)}}{\partial t} + v \frac{\partial f^{(0)}}{\partial x} \right) \right\rangle = \int_0^\infty \int_{-\infty}^\infty \left\{ 1 + \ln f^{(0)} - 2\beta I \frac{(5-3\gamma)}{(3-\gamma)} \right\} \left(\frac{\partial f^{(0)}}{\partial t} + v \frac{\partial f^{(0)}}{\partial x} \right) dv\, dI = 0 \tag{44}$$

On simplifying , eq. (44) can be expressed as

$$\int_0^\infty \int_{-\infty}^\infty \left(\frac{\partial}{\partial t} + v \frac{\partial}{\partial x} \right) \left[f^{(0)} \ln f^{(0)} + \frac{(5-3\gamma)}{2(\gamma-1)} f^{(0)} \ln \beta \right] dv\, dI = 0 \tag{45}$$

The above equation can be expressed in the following compact form

$$\frac{\partial}{\partial t}\left(H^{(0)} \right) + \frac{\partial}{\partial x}\left(H_v^{(0)} \right) = 0 \tag{46}$$

where the functionals $H^{(0)}$ and $H_v^{(0)}$ are defined in (47) and (48) as:

$$H^{(0)} = \int_0^\infty \int_{-\infty}^\infty \left[f^{(0)} \ln f^{(0)} + \frac{(5-3\gamma)}{2(\gamma-1)} f^{(0)} \ln \beta \right] dv\, dI \tag{47}$$

[2] It can be shown that the moments of the BGK-Boltzmann equation with any linear combination of the collision invariants equals zero. Hence the need to express equation (36) as a linear combination of collision invariants.

$$H_v^{(0)} = \int_0^{\infty}\int_{-\infty}^{\infty} v\left[f^{(0)}\ln f^{(0)} + \frac{(5-3\gamma)}{2(\gamma-1)} f^{(0)}\ln\beta\right] dv\, dI \tag{48}$$

On evaluating the moments in eq. (47) the following expression is obtained for $H^{(0)}$

$$H^{(0)} = \rho\left[\ln\rho + \frac{\ln\beta}{(\gamma-1)} - \mathcal{C}_o\right] \tag{49}$$

On comparing eq(s). (49) and (38),

$$\boxed{\rho s = -RH^{(0)}}^{3} \tag{50}$$

The additive constant $\mathcal{C}_o$ is a function of the specific heat ratio γ and the gas constant R. The definition of the H-function can be extended to any distribution function. Accordingly the functionals H and H_v are defined as shown in eq(s). (51) and (52).

$$H = \int_0^{\infty}\int_{-\infty}^{\infty}\left[f\ln f + \frac{(5-3\gamma)}{2(\gamma-1)} f\ln\beta\right] dv\, dI \tag{51}$$

$$H_v = \int_0^{\infty}\int_{-\infty}^{\infty} v\left[f\ln f + \frac{(5-3\gamma)}{2(\gamma-1)} f\ln\beta\right] dv\, dI \tag{52}$$

It can be seen that the expression for H reduces to the classical definition $H = \int_0^{\infty}\int_{-\infty}^{\infty} f\ln f\, dv\, dI$, for the specific case of a monoatomic gas (i.e. $\gamma = 5/3$). For a spatially inhomogenous gas Grad[8] has shown that the following inequality must be satisfied when the gas approaches equilibrium.

[3] This relation establishes a link between Boltzmann's H-Theorem and the classical thermodynamics concept of entropy. It must be pointed out that there is no rigorous justification to extend this definition to include H-functions derived from higher-order distribution functions.

$$\boxed{\frac{\partial}{\partial t}(H)+\frac{\partial}{\partial x}(H_v)\le 0} \tag{53}$$

The above inequality will be shown to be true for the first and second-order distribution functions. The first and second order distribution functions are given by expressions (54) and (55).

$$f = f^{(0)} + \xi f^{(0)}\Phi^{(1)} = f^{(0)}\left(1+\xi\Phi^{(1)}\right) \tag{54}$$

$$f = f^{(0)} + \xi f^{(0)}\Phi^{(1)} + \xi^2 f^{(0)}\Phi^{(2)} = f^{(0)}\left(1+\xi\Phi^{(1)} + \xi^2\Phi^{(2)}\right) \tag{55}$$

On expressing $\ln(f)$ as a Taylor series and considering only terms up to the second power in the Knudsen number the following approximations are obtained for the first and second order distribution functions.

$$\ln\left[f^{(0)}\left(1+\xi\Phi^{(1)}\right)\right] \equiv \ln f^{(0)} + \xi\Phi^{(1)} - \frac{\xi^2\left[\Phi^{(1)}\right]^2}{2} \tag{56}$$

$$\ln\left[f^{(0)}\left(1+\xi\Phi^{(1)}+\xi^2\Phi^{(2)}\right)\right] \equiv \ln f^{(0)} + \left(\xi\Phi^{(1)}+\xi^2\Phi^{(2)}\right) - \frac{\xi^2\left[\Phi^{(1)}+\xi\Phi^{(2)}\right]^2}{2} \tag{57}$$

The H-Balance Equation for the Boltzmann equation is obtained by evaluating the moments in the following equation.

$$\frac{\partial}{\partial t}(H)+\frac{\partial}{\partial x}(H_v) = \int_0^{\infty}\int_{-\infty}^{\infty} v\left(f^{(0)}-f\right)\left[1+\ln f - \frac{2(5-3\gamma)}{(3-\gamma)}\beta I\right] dv\, dI \tag{58}$$

On substituting eq(s). (54) and (56) in the above equation and retaining only terms up to the first power in ξ (Knudsen number) the right hand side (RHS) of the above equation takes the form:

$$\int_0^{\infty}\int_{-\infty}^{\infty} -\nu\xi f^{(0)}\Phi^{(1)}\left[1+\ln f-\frac{2(5-3\gamma)}{(3-\gamma)}\beta I\right] dv\, dI \tag{59}$$

The above integral equals zero as moments of the first-order distribution function with a linear combination[4] of the collision invariants are being evaluated. Since the first-order distribution function satisfies the property $\left\langle \Psi;\ \xi f^{(0)}\Phi^{(1)}\right\rangle = 0$, eq. (54) equals zero. Hence the first -order distribution function satisfies Boltzmann's H-Theorem. On evaluating eq. (58) up to the second power in ξ, the RHS of the equation takes the following form:

$$\begin{aligned}&-\int_0^{\infty}\int_{-\infty}^{\infty}\left\{\xi f^{(0)}\Phi^{(1)}+\xi f^{(0)}\Phi^{(1)}\ln f^{(0)}-\xi f^{(0)}\Phi^{(1)}\frac{2(5-3\gamma)}{(3-\gamma)}\beta I+\xi^2 f^{(0)}\left[\Phi^{(1)}\right]^2\right\} dv\, dI \\ &-\int_0^{\infty}\int_{-\infty}^{\infty}\xi^2 f^{(0)}\Phi^{(2)}\left\{1+\ln f^{(0)}-\frac{2(5-3\gamma)}{(3-\gamma)}\beta I\right\} dv\, dI\end{aligned} \tag{60}$$

The second integral equals zero as the second-order distribution function satisfies the moment property $\left\langle \Psi;\ \xi^2 f^{(2)}\right\rangle = \left\langle \Psi;\ \xi^2 f^{(0)}\Phi^{(2)}\right\rangle = 0$. For reasons given earlier moments of the second-order term with any linear combination of the collision invariants equals zero. Hence eq. (60) simplifies to the following :

$$-\int_0^{\infty}\int_{-\infty}^{\infty}\xi^2 f^{(0)}\left[\Phi^{(1)}\right]^2 dv\, dI \tag{61}$$

On substituting for $\Phi^{(1)}$ from eq. (8) and evaluating the moments

[4] Moments of the first and second-order distribution function with any linear combination of the collision invariants equals zero.

$$-\int_{0}^{\infty}\int_{-\infty}^{\infty}\xi^2 f^{(0)}\left[\Phi^{(1)}\right]^2 \, dv \, dI = -\frac{1}{\nu^2}\left[\frac{5\rho}{4\beta^3}\left(\frac{\partial\beta}{\partial x}\right)^2 + \frac{\left(3\gamma^2 - 10\gamma + 11\right)}{2}\left(\frac{\partial u}{\partial x}\right)^2\right] \qquad (62)$$

It must be noted that eq. (57) is always less than zero. Hence the second-order distribution function satisfies Boltzmann's H-Theorem. It has been proved conclusively that both the first and second-order distribution functions satisfy the inequality

$$\boxed{\frac{\partial}{\partial t}(H) + \frac{\partial}{\partial x}(H_v) \le 0}$$

As a consequence the BGK-Burnett equations which are obtained from the BGK-Boltzmann equation by using the second-order distribution function are entropy consistent !

NUMERICAL EXPERIMENTS

The BGK-Burnett equations were numerically integrated using a hybrid algorithm for the hypersonic shock structure problem. In the hybrid algorithm the inviscid fluxes were split using the KWPS scheme and the viscous and BGK-Burnett fluxes were central differenced. The objective of this experiment was to test the computational stability of the entropy consistent BGK-Burnett equations by integrating them numerically on progressively finer grids. In order to test the stability of the algorithm, the scheme was applied initially to a coarse mesh of 101 grid points. The number of grid points was increased to 501. The reference parameters used for Argon are similar to those used by Zhong[4]. The results of the computations are shown in Fig(s) 5-12. Fig(s) 5-8 compare the entropy plots of the BGK-Burnett equations with the entropy plots of the Burnett equations of Fiscko and Chapman[3]. Fig(s) 9-12 compare the normalized temperature and specific entropy profiles of the BGK-Burnett and Navier-Stokes equations.

CONCLUSIONS

An entropy consistent set of BGK-Burnett equations has been derived from first principles. These equations have been numerically integrated to compute the hypersonic shock structure. The equations are computationally stable for the range of grid points and Knudsen numbers for which results are presented.

PROPOSED RESEARCH

An attempt is being made to compare the expressions for entropy balance obtained from kinetic theory (Boltzmann's H-Theorem) and classical thermodynamics, and account for the differences between the two expressions. Since the BGK-Burnett equations in 1-D have been proven to be entropy consistent a similar analysis for 2-D BGK-Burnett equations will be carried out. Numerical solutions for hypersonic flow past blunt bodies will be computed using the 2-D BGK-Burnett equations.

REFERENCES

[1] Comeaux, K. A., Chapman, D. R., and MacCormack, R. W., "An Analysis of the Burnett Equations Based on the Second Law of Thermodynamics," AIAA 95-0415, Reno, NV, 33rd Aerospace Sciences Meeting, January 9-12, 1995.

[2] Balakrishnan R. and Agarwal, R. K., "Entropy Consistent Formulation and Numerical Simulation of BGK-Burnett Equations for Hypersonic Flows Using a Kinetic Wave/Particle Flux Splitting Algorithm", International Conference for Numerical Methods in Fluid Dynamics, 24-28 June, 1996, Monterey, California.

[3] Fiscko, K. A. and Chapman, D. R., "Comparison of Burnett, Super-Burnett and Monte Carlo Solutions for Hypersonic Shock Structure," Proceedings of the 16th International Symposium on Rarefied Gas Dynamics, Pasadena, California, July 11-15, 1988.

[4] Zhong, X., "Development and Computation of Continuum Higher Order Constitutive Relations for High-Altitude Hypersonic Flow," Ph.D. Thesis, Stanford University, 1991.

[5] Welder, W. T., Chapman, D. R., and MacCormack, R. W., "Evaluation of Various Forms of the Burnett Equations," AIAA-93-3094, AIAA 24th Fluid Dynamics Conference, Orlando, FL, July 6-9, 1993.

[6] Balakrishnan R. and Agarwal, R. K., "Formulation of a Second Order Distribution Function by Perturbation Analysis of the Boltzmann Equation," report (unpublished), Department of Aerospace Engineering, Wichita State University, 1995.

[7] Bobylev, A. V., "The Chapman-Enskog and Grad Methods for Solving the Boltzmann Equation", Sov. Phys. Dokl., 27(1), January 1982.

[8] Grad, H. "On the Kinetic Theory of Rarefied Gases", Communications on Pure and Applied Mathematics, Vol. 2, Pages 331-407, 1949.

Burnett and BGK-Burnett Coefficients

Euler equations have been used in the BGK-Burnett equations to express the time derivatives in terms of the spatial derivatives.

Table: 1

Stress and Heat Transfer Coefficients	Fiscko & Chapman (Air) $\gamma = 1.4$	BGK-Burnett (Air) $\gamma = 1.4$	Fiscko & Chapman (Argon) $\gamma = 1.6666$	BGK-Burnett (Argon) $\gamma = 1.6666$
$a^{(1)}$	1.749	0.96	1.749	0.446
$a^{(2)}$	-388.024	-459.2	-281.216	-277.472
$a^{(3)}$	388.024	459.2	281.216	277.472
$a^{(4)}$	-257.726	-5625.0	-186.784	-1216
$a^{(5)}$	403.522	-5166.0	292.448	-938.11
$a^{(6)}$	74.62	-5625	54.08	-1216.0
$b^{(1)}$	10.831	-21.633	10.831	-9.896
$b^{(2)}$	-2.269	0.183	-2.269	-0.194
$b^{(3)}$	-2.06	0.533	-2.06	-0.443

Augmented Burnett and BGK-Burnett Stress Coefficients

Navier-Stokes equations have been used to express the time derivatives in terms of the spatial derivatives.

Table: 2

Stress Coefficients	Zhong (Air) $\gamma = 1.4$	BGK-Burnett (Air) $\gamma = 1.4$	Zhong (Argon) $\gamma = 1.6666$	BGK-Burnett (Argon) $\gamma = 1.6666$
$a^{(1)}$	1.749	0.96	1.749	0.446
$a^{(2)}$	-388.024	-459.2	-281.216	-277.472
$a^{(3)}$	388.024	459.2	281.216	277.472
$a^{(4)}$	-257.726	-5625	-186.784	-1216
$a^{(5)}$	403.522	-5166	292.448	-938.11
$a^{(6)}$	74.62	-5625	54.08	-1216
$a^{(7)}$	0	-459.2	0	-277.472
$a^{(8)}$	0	642.88	0	462.268
$a^{(9)}$	63.778	459.2	46.222	277.472
$a^{(10)}$	0	0.64	0	0.888

Augmented Burnett and BGK-Burnett Heat Transfer Coefficients

Navier-Stokes equations have been used to express the time derivatives in terms of the spatial derivatives.

Table: 3

Heat Transfer Coefficients	Zhong (Air)	BGK-Burnett (Air)	Zhong (Ar)	BGK-Burnett (Ar)
$b^{(1)}$	10.831	-21.633	10.831	-9.896
$b^{(2)}$	-2.269	0.183	-2.269	-0.194
$b^{(3)}$	-2.06	0.533	-2.06	-0.443
$b^{(4)}$	0	4.4	0	4.666
$b^{(5)}$	0	1406	0	866.84
$b^{(6)}$	0	-1406	0	-866.84
$b^{(7)}$	-2186	1406	-2041	866.84
$b^{(8)}$	0	0.7	0	0.833
$b^{(9)}$	0	-1.4	0	-1.666
$b^{(10)}$	0	-22500	0	-13870
$b^{(11)}$	-179.375	0	-130	0

Fig. 1 Linearized Stability Analysis†

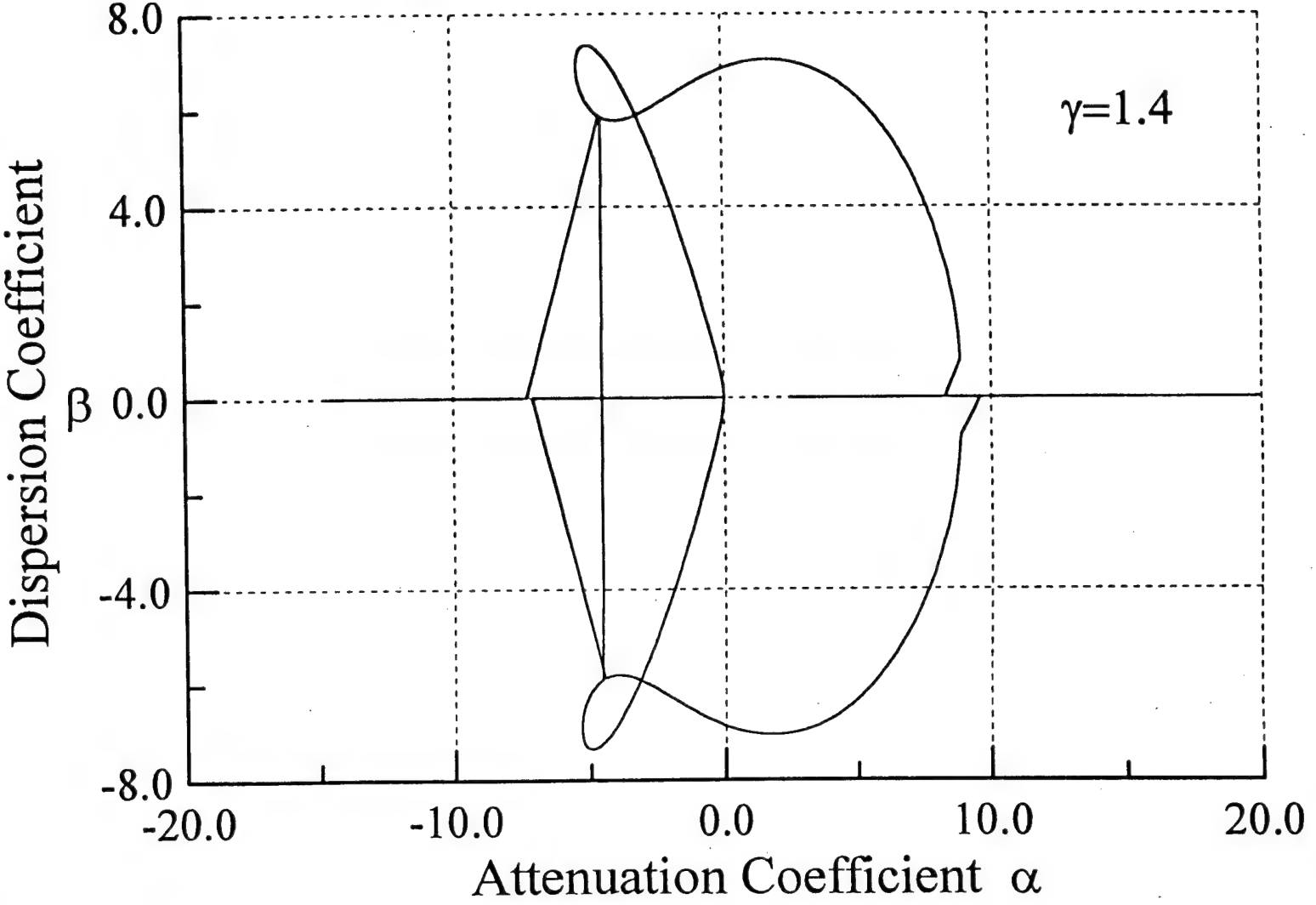

† Euler equations have been used to express the material derivatives in terms of the spatial derivatives.

Fig. 2 Linearized Stability Analysis†

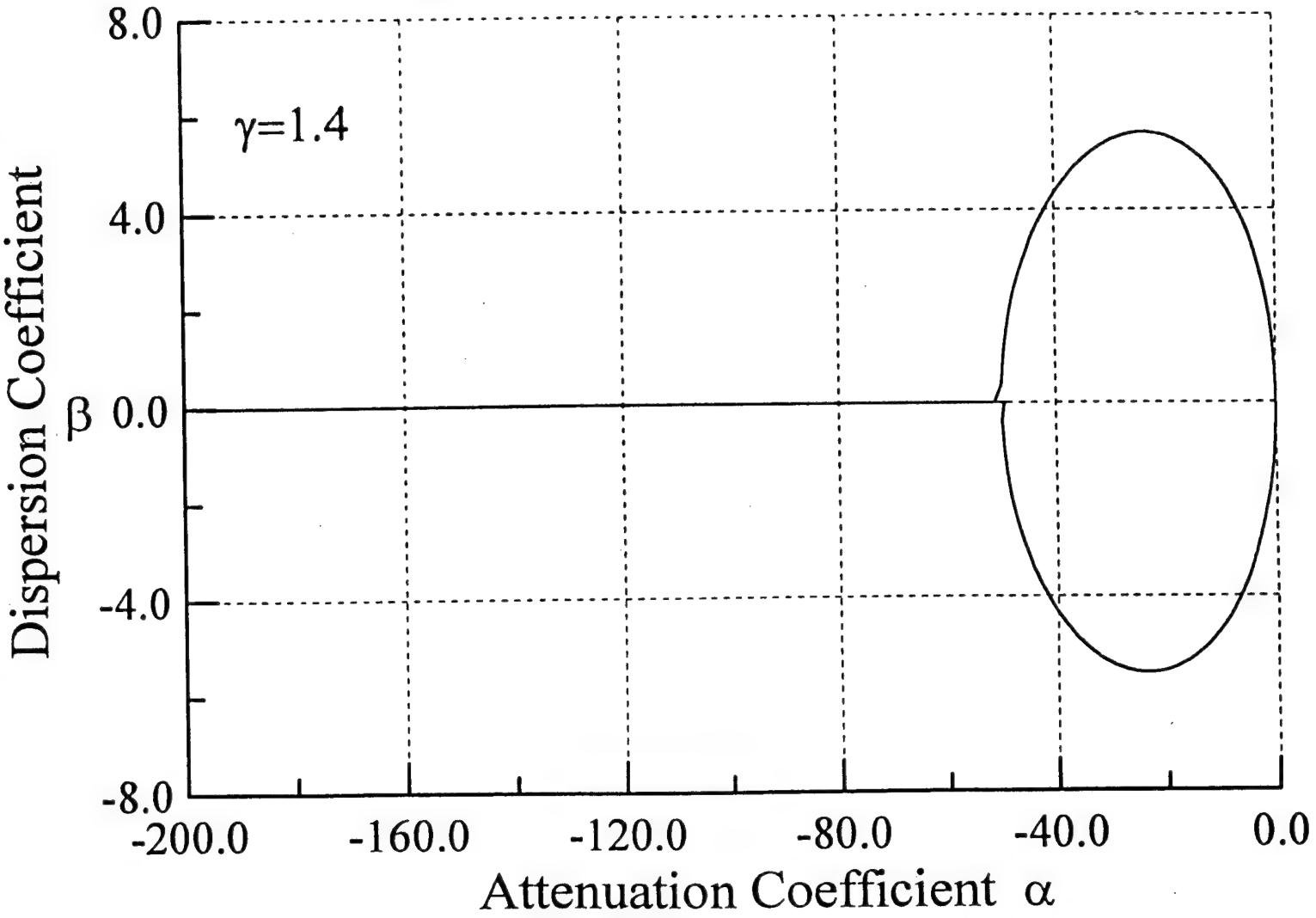

† Navier-Stokes equations have been used to express the material derivatives in terms of the spatial derivatives.

Fig. 3 Linearized Stability Analysis†

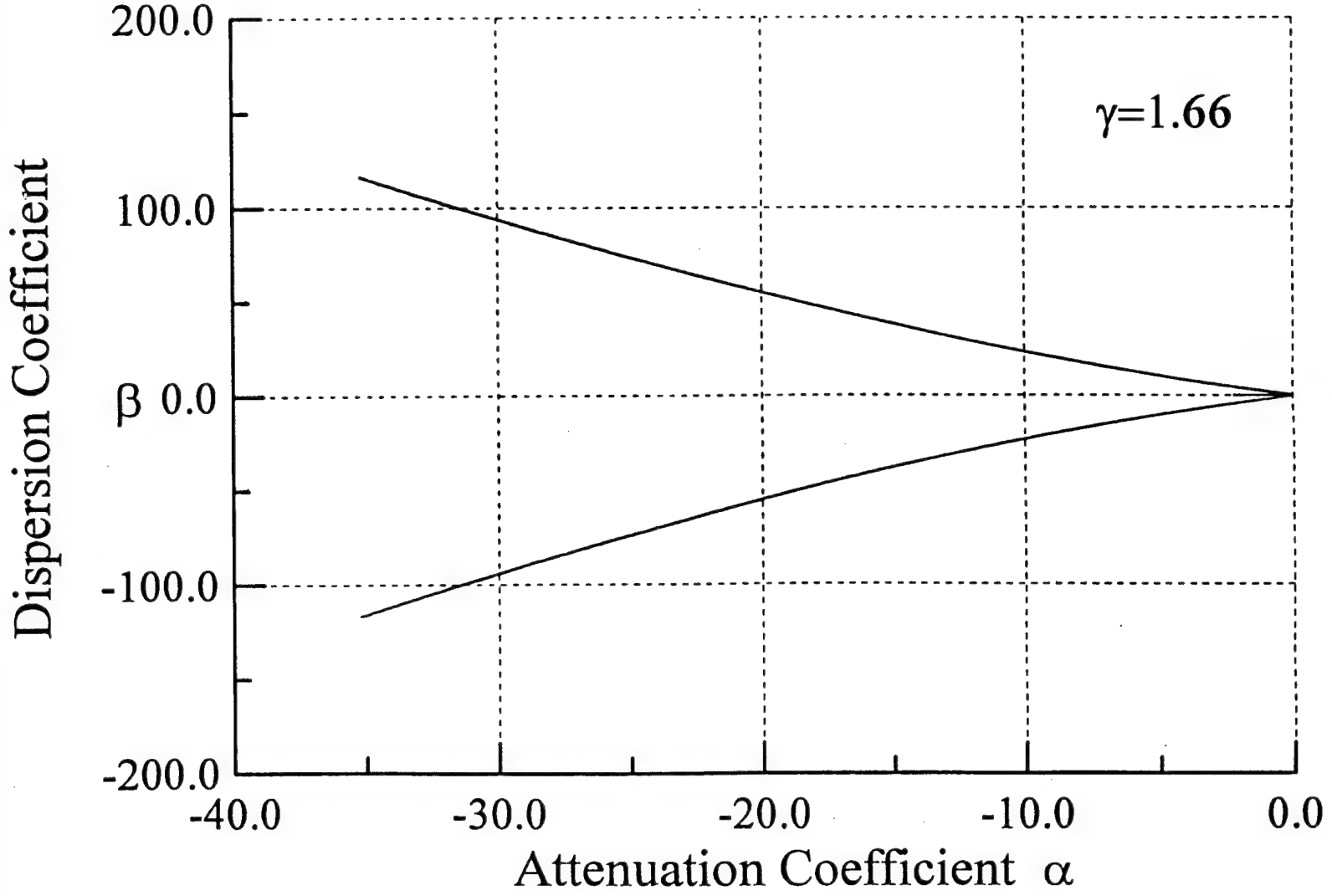

† Euler equations have been used to express the material derivatives in terms of the spatial derivatives

Fig. 4 Linearized Stability Analysis†

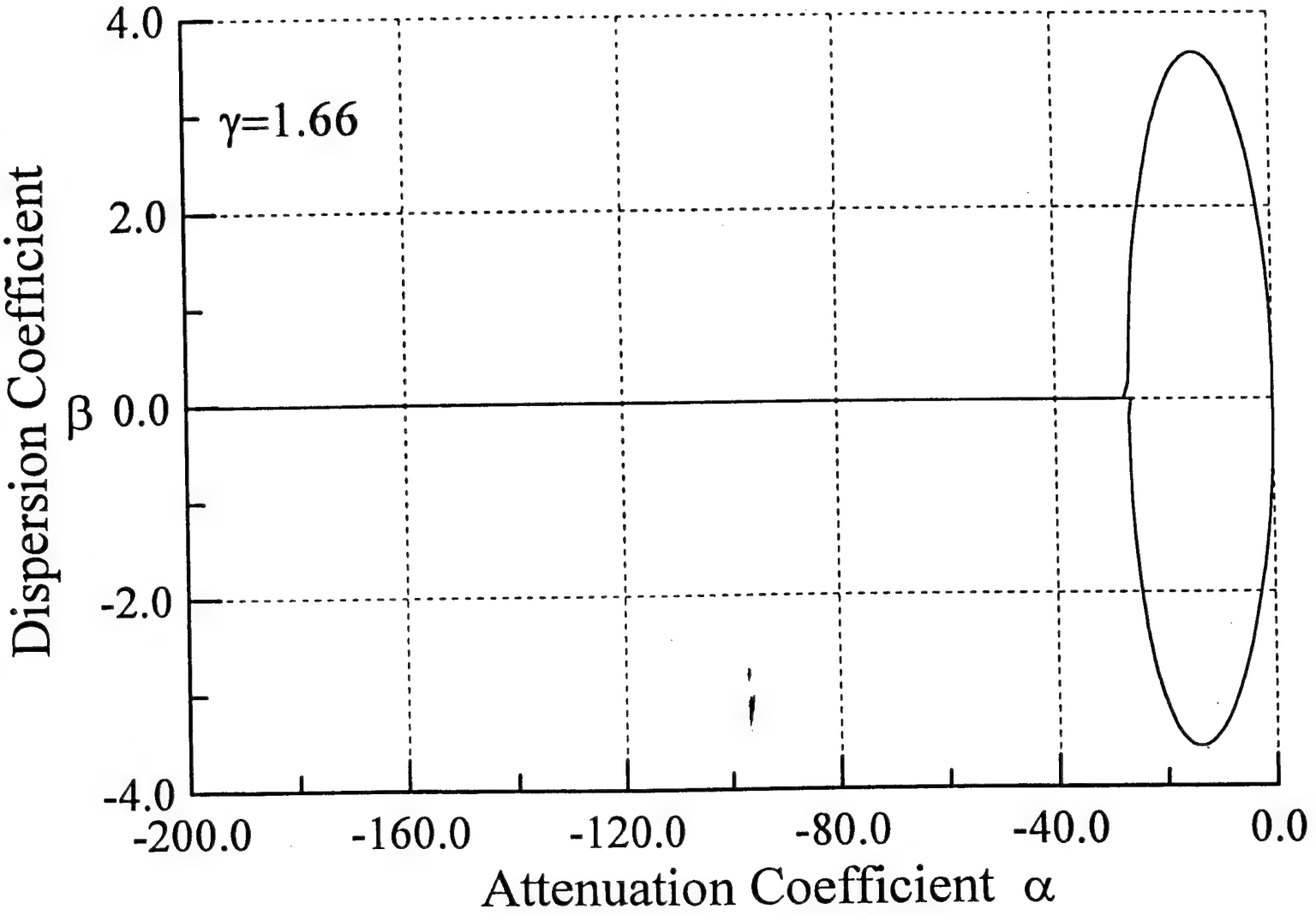

† Navier-Stokes equations have been used to express the material derivatives in terms of the spatial derivatives

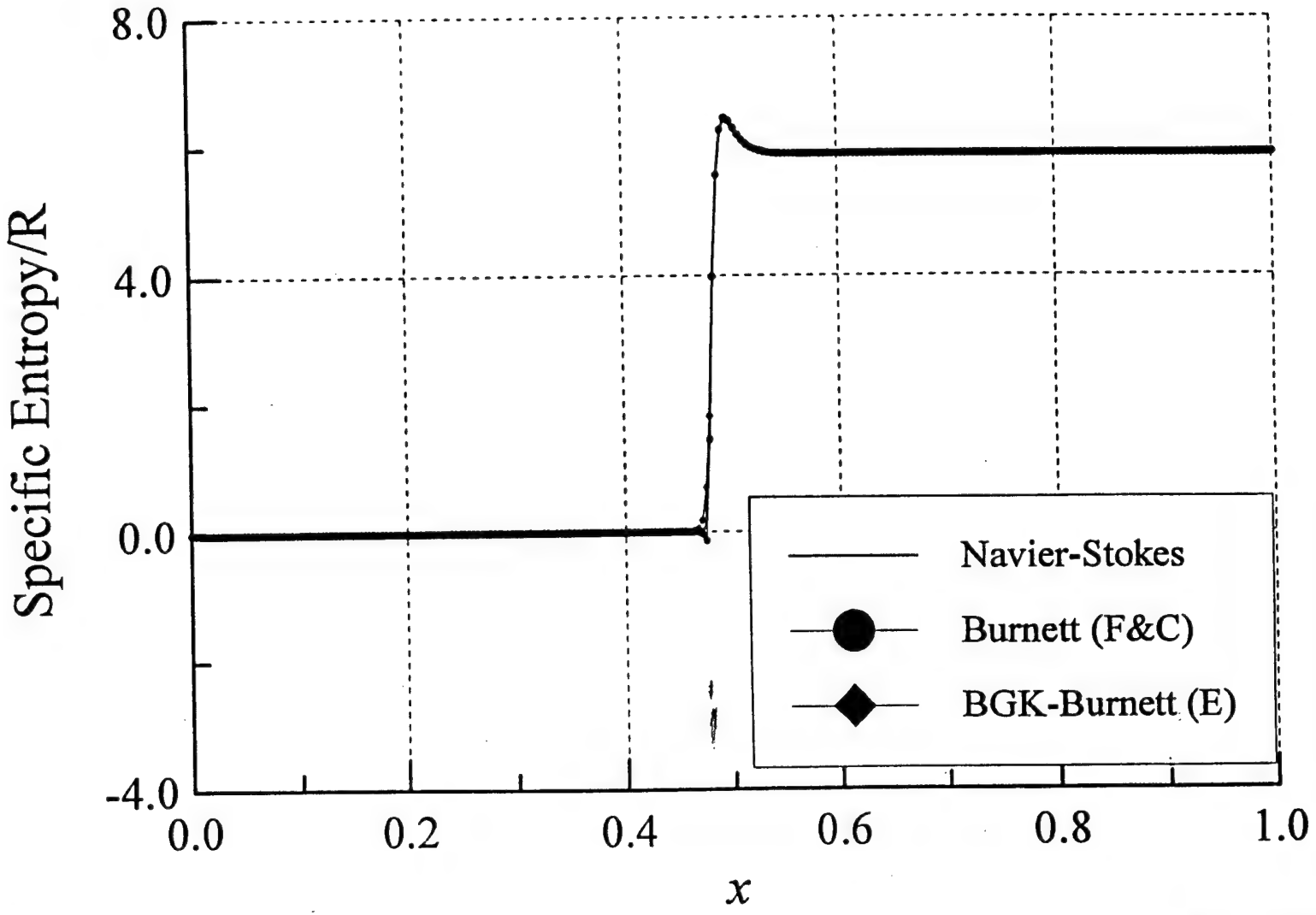

Fig. 5 Specific entropy variation across a Mach 20 normal shock (Argon). Kn_∞=0.0005

Euler equations have been used to express the material derivatives in terms of the spatial derivatives.

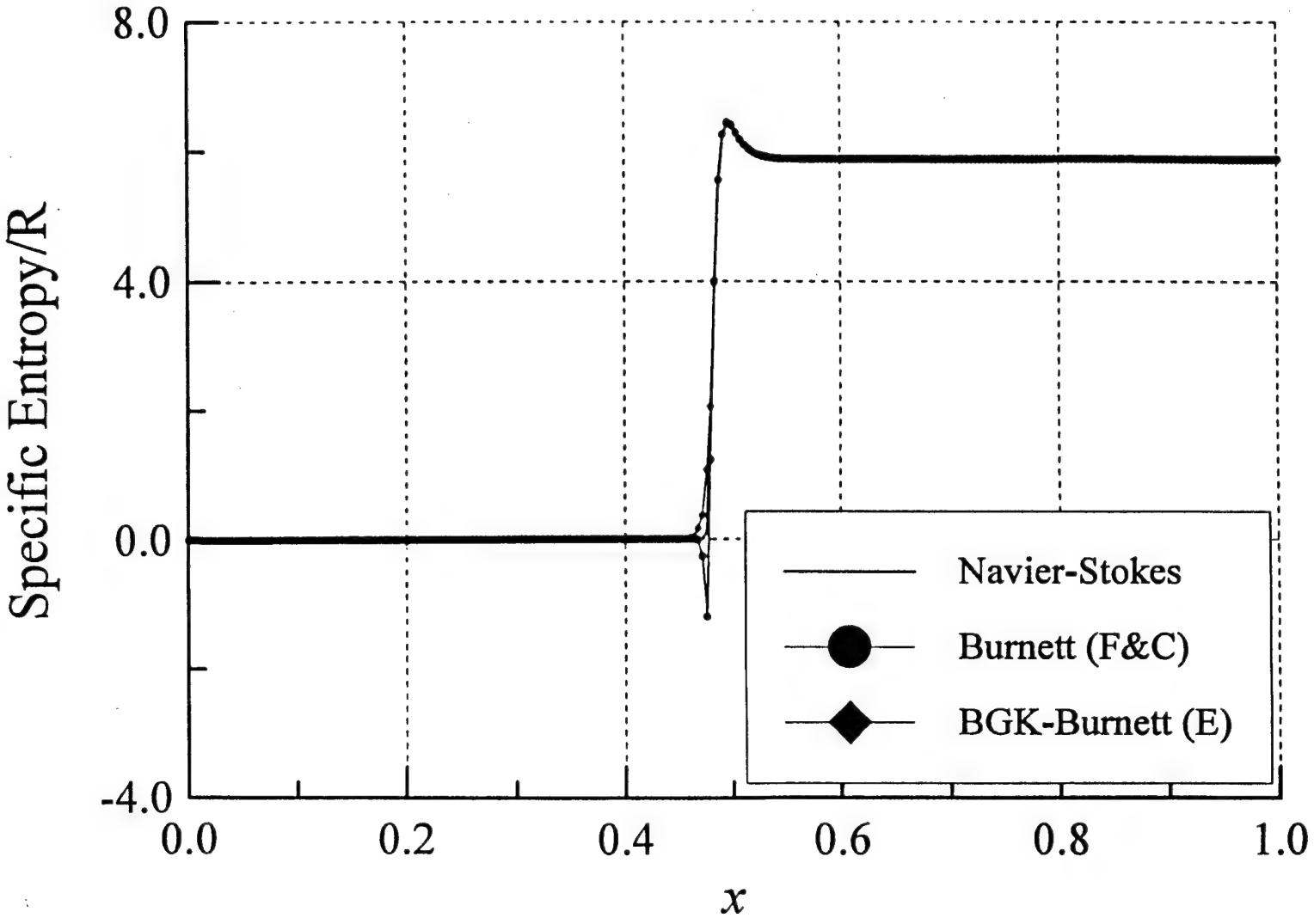

Fig.6 Specific entropy variation across a Mach 20 normal shock (Argon), Kn_∞=0.001

Euler equations have been used to express the material derivatives in terms of the spatial derivatives.

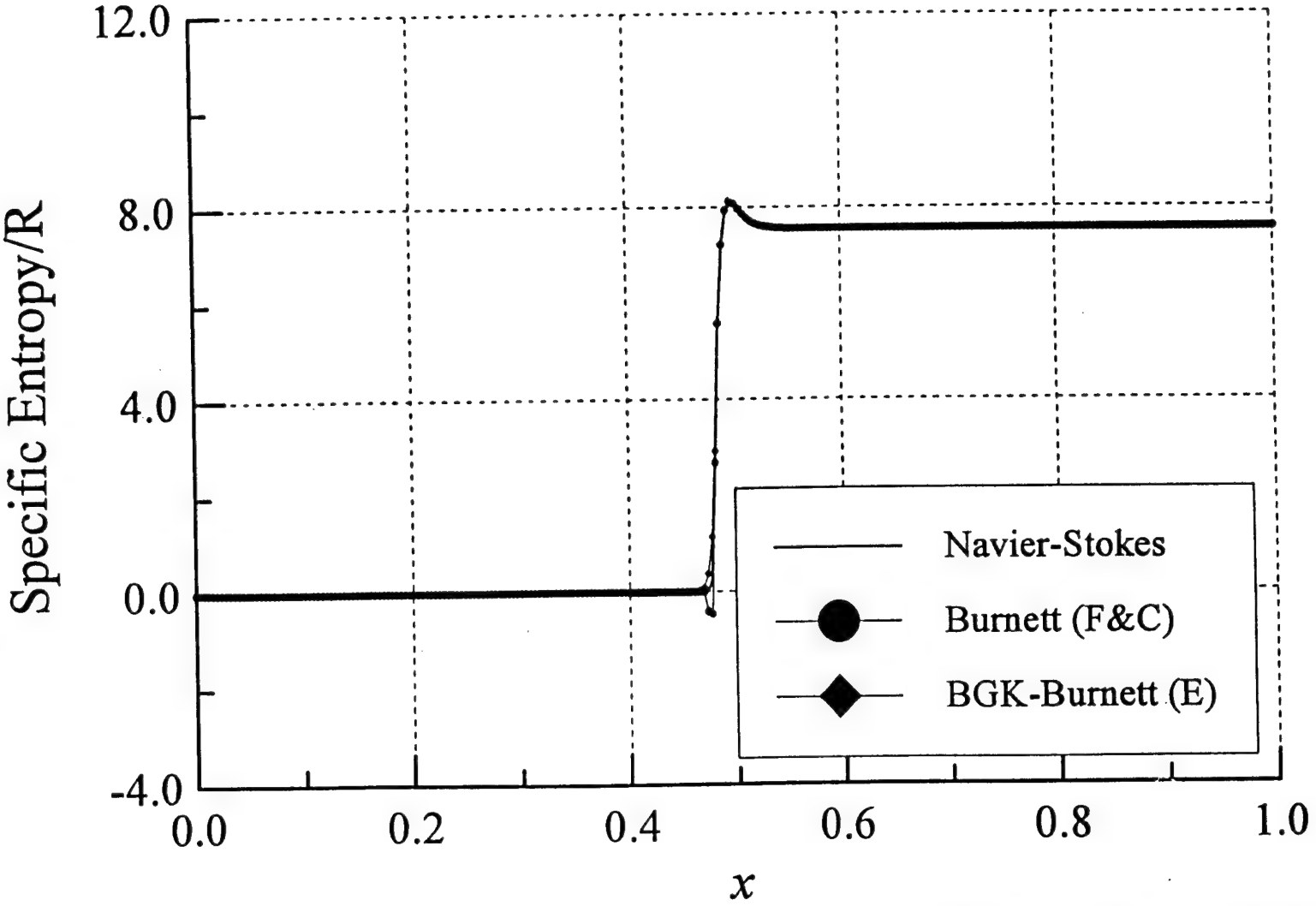

Fig. 7 Entropy variation across a Mach 35 normal shock (Argon). $Kn_\infty = 0.0005$

Euler equations have been used to express the material derivatives in terms of the spatial derivatives.

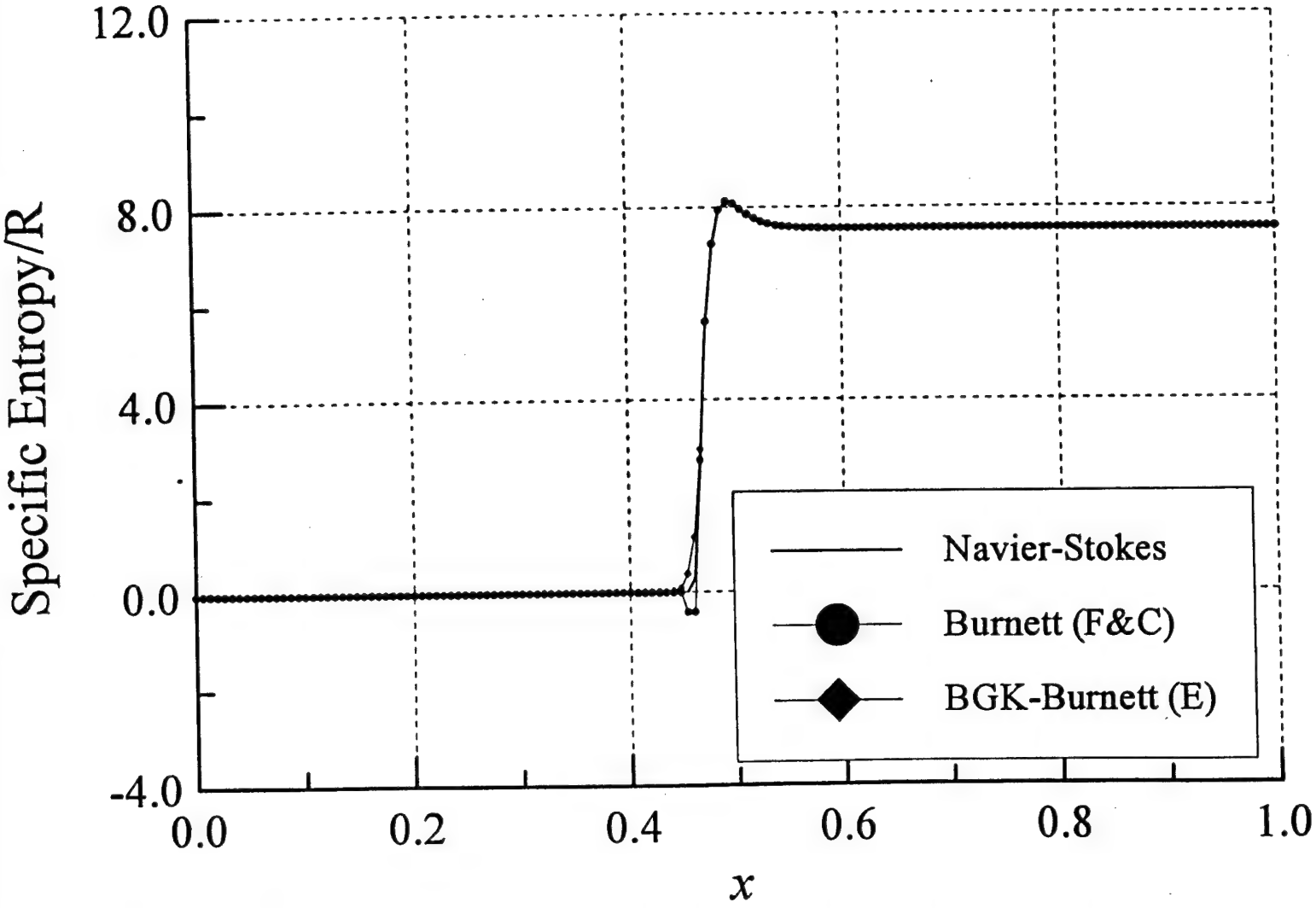

Fig. 8 Entropy variation across a Mach 35 normal shock (Argon). $Kn_\infty = 0.001$

Euler equations have been used to express the material derivatives in terms of the spatial derivatives

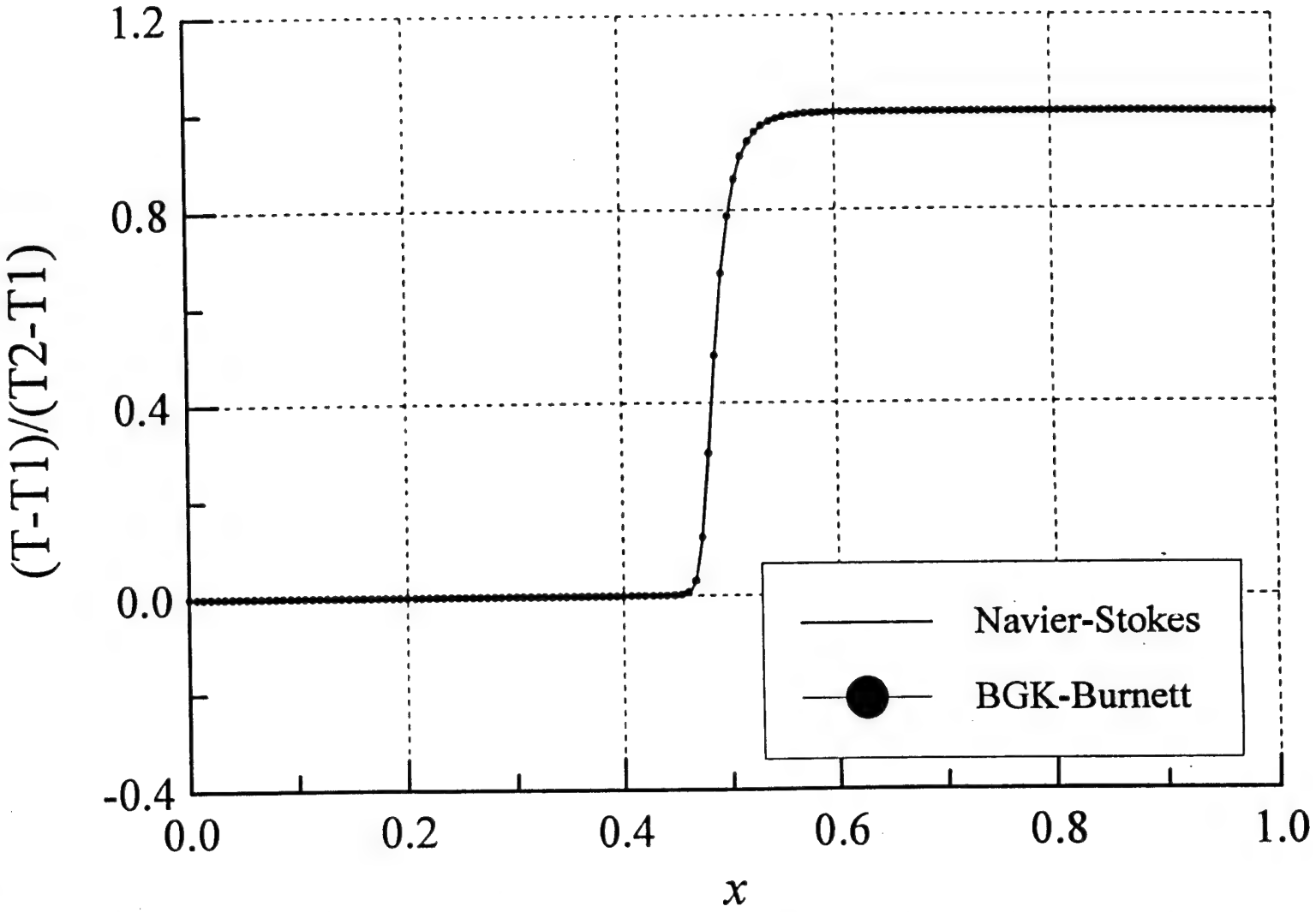

Fig. 9 Temperature variation across a Mach 35 normal shock (Argon). $Kn_\infty = 0.01$

Navier-Stokes equations have been used to express the material derivatives in terms of the spatial derivatives.

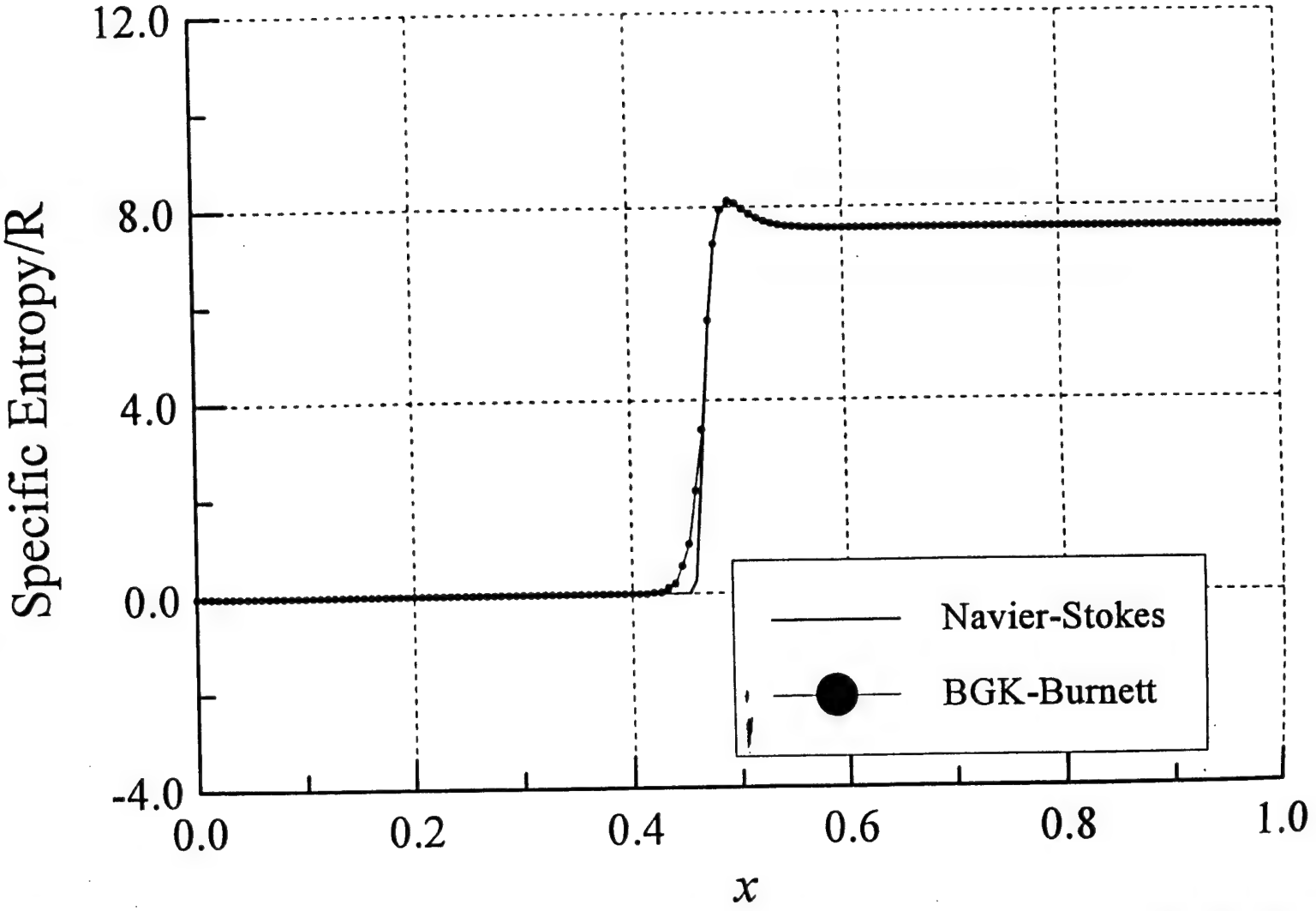

Fig. 10 Specific entropy variation across a Mach 35 normal shock (Argon). $Kn_\infty = 0.01$

Navier-Stokes equations have been used to express the material derivatives in terms of the spatial derivatives

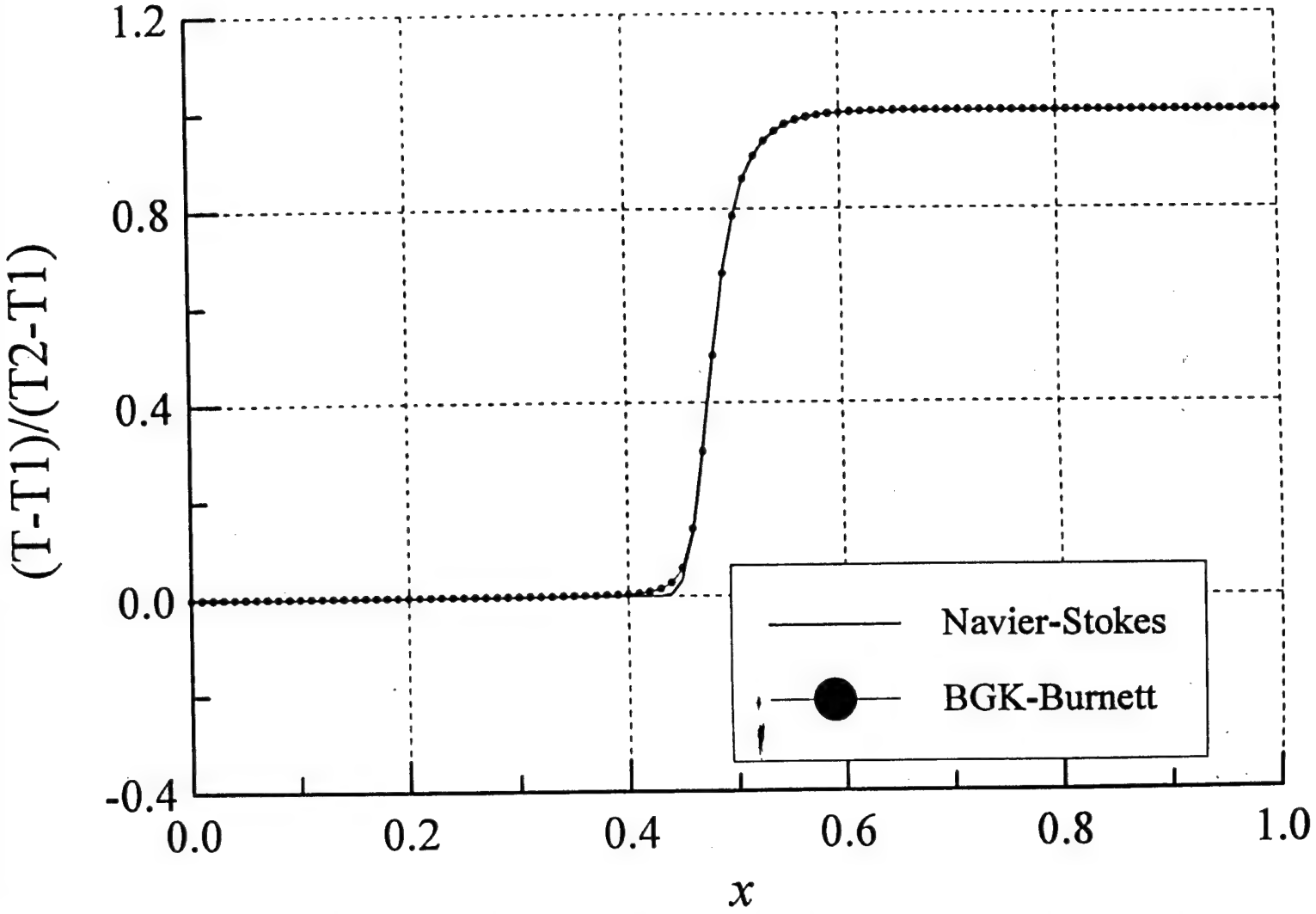

Fig. 11 Temperature variation across a Mach 35 normal shock (Argon). $Kn_\infty = 0.02$

Navier-Stokes equations have been used to express the material derivatives in terms of the spatial derivatives.

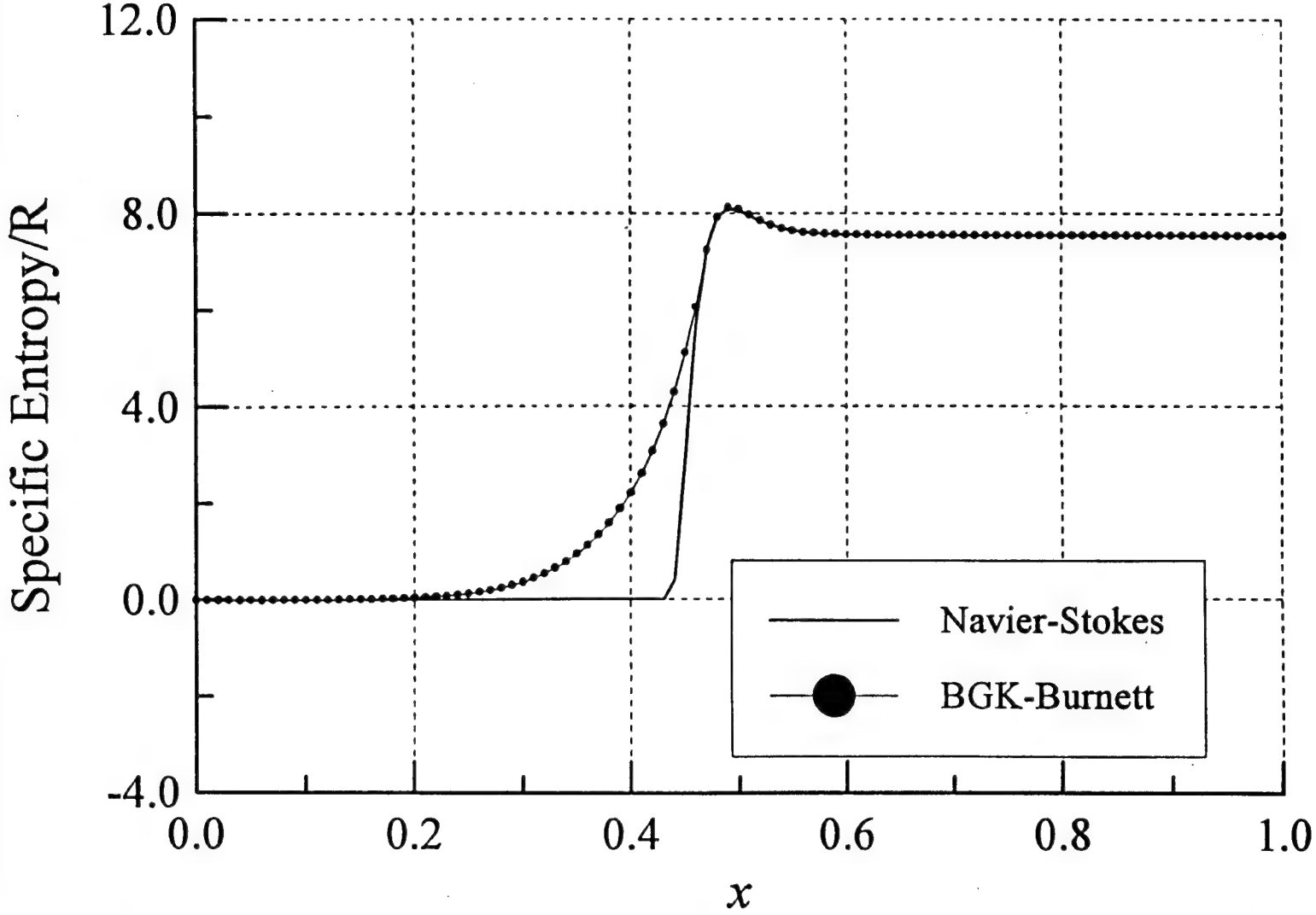

Fig. 12 Specific entropy variation across a Mach 35 normal shock (Argon). $Kn_\infty = 0.02$

Navier-Stokes equations have been used to express the material derivatives in terms of the spatial derivatives.

Appendix: One

The expressions for the coefficients in the BGK-Burnett flux vector are given below:

$$\omega_1 = \frac{4\gamma}{9-7\gamma},\ \omega_2 = \frac{2\gamma}{9-7\gamma},\ \omega_3 = -\left(\frac{2}{3}\right)(3-\gamma)$$

$$\theta_1 = 2.5 + \omega_1,\ \theta_2 = \omega_2 - 1,\ \theta_3 = -(1+\omega_1),\ \theta_4 = (3-\gamma) + \omega_3$$

$$\theta_5 = -\left[(\gamma-1) + \omega_3\right],\ \theta_6 = \left(\frac{3\gamma-5}{2}\right) + \omega_3$$

$$\Omega_1 = \left(\frac{3-\gamma}{2}\right),\ \Omega_2 = \left(\frac{3}{4}\right)\left(\theta_1 + \theta_2 + \frac{5}{2}\theta_3\right),\ \Omega_3 = \frac{\gamma}{4(\gamma-1)}$$

$$\Omega_4 = \frac{1}{8(\gamma-1)}\left\{(6\gamma-3)\theta_4 + (\gamma+3)\theta_5 + 2\gamma\theta_6\right\}$$

The coefficients of the stress and heat transfer terms are given below:

$$a^{(1)} = 2(2-\gamma)\Omega_1,\ a^{(2)} = -2\Omega_1 R,\ a^{(3)} = 2\Omega_1 R,\ a^{(4)} = -4\left(\frac{\Omega_1}{2} + \Omega_2\right)R,\ a^{(5)} = -4\Omega_2 R$$

$$a^{(6)} = -4\left(\frac{\Omega_1}{2} + \Omega_2\right)R,\ a^{(7)} = -2\Omega_1 R,\ a^{(8)} = 2R\gamma\Omega_1,\ a^{(9)} = 2\Omega_1 R,\ a^{(10)} = 2(\gamma-1)\Omega_1$$

$$b^{(1)} = 8\Omega_4 - 4\Omega_3(2\gamma - 1) - 4\Omega_2 - 2\Omega_1,\ b^{(2)} = \Omega_4 - \Omega_3(\gamma - 1),\ b^{(3)} = 4\Omega_4 - 2\Omega_1$$

$$b^{(4)} = 2\left(\Omega_1 + 4\Omega_3(\gamma - 1)\right),\ b^{(5)} = 4\gamma\Omega_3 R,\ b^{(6)} = -4\gamma\Omega_3 R,\ b^{(7)} = 4\gamma\Omega_3 R$$

$$b^{(8)} = 2\Omega_3(\gamma - 1),\ b^{(9)} = -4\Omega_3(\gamma - 1),\ b^{(10)} = -64\gamma\Omega_3 R$$

A Comparative Study of Augmented Burnett and BGK-Burnett Equations for Computing Hypersonic Blunt Body Flow

Project Report

Prepared for

Air Force Office of Scientific Research
Directorate of Aerospace Sciences
AFOSR/NA
Bolling AFB
Washington DC 20332-6448

Principal Investigator
Dr. Ramesh K. Agarwal

Graduate Research Assistant
Keon-Young Yun

Department of Aerospace Engineering
Wichita State University
Wichita, Kansas 67206-0044

September, 1996

Table of Contents

Abstract

In this paper two different forms of Burnett equations are studied which have been designated as 'Augmented Burnett Equations' and 'BGK-Burnett Equations'. The augmented Burnett equations were developed by Zhong to stabilize the solution of the conventional Burnett equations which were derived in 1935 by Burnett from the Boltzmann equation using the second-order Chapman-Enskog expansion. In this formulation, The conventional Burnett equations are augmented by adding *ad hoc* third-order derivatives to stress and heat transfer terms so that the augmented equations are stable to small wavelength disturbances. The BGK-Burnett equations have been recently derived by Agarwal and Balakrishnan from the Boltzmann equation using the Bhatnagar-Gross-Krook (BGK) approximation for the collision integral. These equations have been shown to be entropy consistent and satisfy the Boltzmann H-Theorem in contrast to the conventional Burnett equations which violate the second law of thermodynamics. In this paper, both sets of Burnett equations are applied to compute a 2-D hypersonic flow over a circular cylinder at Knudsen numbers 0.001 to 0.1. The radius of the cylinder, which is the characteristic length of the body, determines the Knudsen number. The Steger-Warming flux-vector splitting scheme is applied to the convective inviscid flux terms. Stress and heat transfer terms are simply second-order central-differenced. Comparison is made between the augmented and BGK-Burnett equations solutions and with the Navier-Stokes calculations. Comparison of the solutions from the augmented Burnett equations with the Navier-Stokes solutions shows that the difference is significant at high Knudsen number (Kn=0.1). The solutions from the BGK-Burnett equations are matched well with those from the Navier-Stokes equations and the augmented Burnett equations at lower Knudsen numbers (Kn=0.001, 0.01). BGK-Burnett solutions are currently underway at higher Knudsen numbers.

Nomenclature

e_t	total energy
Kn	Knudsen number
M	Mach number
Pr	Prandtl number
p	pressure
q_i	heat flux
Re	Reynolds number
R	gas constant
T	temperature
T_w	wall temperature
t	time
u, v	velocity components in x, y, z direction

Greek symbols

α_k, β_k	coefficients of stress terms in Burnett equations
γ_i	coefficients of heat flux terms in Burnett equations
δ_i	coefficients of stress terms in Navier-Stokes equations
θ_i	coefficients of third order terms in BGK Burnett equations
κ	thermal conductivity
μ	coefficient of viscosity
ρ	density
σ_{ij}	stress tensor
γ	specific heat ratio

Superscript

(a)	third order terms in augmented Burnett equations
(B)	third order terms in BGK Burnett equations

Subscripts

x, y	derivatives in x and y directions
∞	free stream quantities

1. Introduction

In one of the first attempts to solve the Burnett equations, Fiscko and Chapman[1] solved the hypersonic shock structure problem for a variety of Mach numbers and concluded that the Burnett equations describe the normal shock structure better than the Navier-Stokes equations at high Mach numbers. However, in their numerical solution, they experienced stability problems on finer grids. The linearized Burnett equations were found to be unstable to small wavelength disturbances. In a subsequent attempt, Zhong[2] stabilized the Burnett equations by adding a few linear third order terms on an *ad hoc* basis. This set of equations was termed the augmented Burnett equations. The augmented Burnett equations did not present stability problems when they were applied to the hypersonic shock structure and hypersonic blunt body problems. However the augmented Burnett equations were not entirely successful to compute the flowfields for blunt body wakes and flat plate boundary layers. Comeaux et. al[3] have noted that the linear stability analysis is not sufficient to explain the instability of the Burnett equations with increasing Knudsen numbers because of many non-linear terms present in the Burnett equations. They have conjectured that this instability may be due to the fact that the Burnett equations violate the second law of thermodynamics at high Knudsen numbers.

The highly non-linear nature of the collision integral in the Boltzmann equation is simplified by representing the collision integral in the Bhatnagar-Gross-Krook (BGK) form. Balakrishnan and Agarwal[4] have formulated a new set of entropy consistent 1-D Burnett equations from the BGK-Boltzmann equation and using the Navier-Stokes equations to approximate the material derivatives in the second order terms in the Chapman-Enskog expansion. The material derivatives are thus expressed in terms of spatial derivatives using the Navier-Stokes equations. This set of BGK-Burnett equations contains all the stress and heat flux terms reported by Fiscko and Chapman[1] and has additional terms which are similar to the super Burnett terms. Recently, Balakrishnan and Agarwal[5] have extended the 1-D BGK-Burnett equations to 2-D BGK-Burnett equations. In this paper, the augmented Burnett equations[2] and the 2-D BGK-Burnett equations[5] have been used to compute and compare the shock structure and other flow properties for hypersonic flow over a blunt body in continuum-transition regime.

2. Governing Equations

The governing equations for 2-D compressible viscous flow in Cartesian coordinates are

$$\frac{\partial Q}{\partial t}+\frac{\partial E}{\partial x}+\frac{\partial F}{\partial y}=0, \tag{1}$$

where

$$Q=\begin{bmatrix}\rho\\ \rho u\\ \rho v\\ e_t\end{bmatrix}. \tag{2}$$

E and F are the flux vectors of the conserved variables Q in the x and y directions. These flux vectors can be written as

$$\begin{aligned}E&=E_I+E_V,\\ F&=F_I+F_V,\end{aligned} \tag{3}$$

where E_I and F_I are the inviscid flux terms and E_V and F_V are the viscous flux terms given as follows:

$$E_I=\begin{bmatrix}\rho u\\ \rho u^2+p\\ \rho uv\\ (e_t+p)u\end{bmatrix}, \qquad E_V=\begin{bmatrix}0\\ \sigma_{11}\\ \sigma_{12}\\ \sigma_{11}u+\sigma_{12}v+q_1\end{bmatrix}, \tag{4}$$

$$F_I=\begin{bmatrix}\rho v\\ \rho uv\\ \rho v^2+p\\ (e_t+p)v\end{bmatrix}, \qquad F_V=\begin{bmatrix}0\\ \sigma_{21}\\ \sigma_{22}\\ \sigma_{21}u+\sigma_{22}v+q_2\end{bmatrix}. \tag{5}$$

In Eqs. (4) and (5), the stress tensors and heat flux terms, σ_{ij} and q_i are expressed as follows:

$$\begin{aligned}\sigma_{ij}&=\sigma_{ij}^{(0)}+\sigma_{ij}^{(1)}+\sigma_{ij}^{(2)}+\sigma_{ij}^{(3)}+\cdots+\sigma_{ij}^{(n)}+O(Kn^{n+1}),\\ q_i&=q_i^{(0)}+q_i^{(1)}+q_i^{(2)}+q_i^{(3)}+\cdots+q_i^{(n)}+O(Kn^{n+1}).\end{aligned} \tag{6}$$

The zeroth order approximation (n=0) results in the Euler equations,

$$\sigma_{ij}^{(0)} = 0,$$

and

$$q_i^{(0)} = 0. \tag{7}$$

The first order approximation represents the Navier-Stokes equations. The stress tensors and the heat flux terms (n=1) are given as,

$$\sigma_{11}^{(1)} = -\mu\left(\delta_1 u_x + \delta_2 v_y\right),$$
$$\sigma_{12}^{(1)} = \sigma_{21}^{(1)} = -\mu\left(u_y + v_x\right),$$
$$\sigma_{22}^{(1)} = -\mu\left(\delta_1 v_y + \delta_2 u_x\right),$$
$$q_1^{(1)} = -\kappa T_x,$$

and

$$q_2^{(1)} = -\kappa T_y. \tag{8}$$

where $(\ )_x = \partial/\partial x$ and $(\ )_y = \partial/\partial y$. The coefficients, δ_1 and δ_2 are given in Table 1 for the augmented Burnett equations[2] and the BGK-Burnett equations[5].

	Aug. Burnett Eqns.	BGK-Burnett Eqns. $\gamma = 1.4$	BGK-Burnett Eqns. $\gamma = 1.666$
δ_1	1.333	1.6	1.333
δ_2	-0.666	-0.4	-0.666

Table 1. The coefficients in the Navier-Stokes Eqns. stress tensors.

Similarly, the second order approximation represents the Burnett equations. The expression for stress and heat flux terms (n=2) are,

$$\begin{aligned}\sigma_{11}^{(2)} = \frac{\mu^2}{p}\Big(& \alpha_1 u_x^2 + \alpha_2 u_x v_y + \alpha_3 v_y^2 + \alpha_4 u_y v_x + \alpha_5 u_y^2 + \alpha_6 v_x^2 \\ & + \alpha_7 RT_{xx} + \alpha_8 RT_{yy} + \alpha_9 \frac{RT}{\rho}\rho_{xx} + \alpha_{10}\frac{RT}{\rho}\rho_{yy} \\ & + \alpha_{11}\frac{RT}{\rho^2}\rho_x^2 + \alpha_{12}\frac{R}{\rho}T_x\rho_x + \alpha_{13}\frac{R}{T}T_x^2 + \alpha_{14}\frac{RT}{\rho^2}\rho_y^2 \\ & + \alpha_{15}\frac{R}{\rho}T_y\rho_y + \alpha_{16}\frac{R}{T}T_y^2\Big),\end{aligned} \tag{9}$$

$$\sigma_{22}^{(2)} = \frac{\mu^2}{p}(\alpha_1 v_y^2 + \alpha_2 u_x v_y + \alpha_3 u_x^2 + \alpha_4 u_y v_x + \alpha_5 v_x^2 + \alpha_6 u_y^2$$
$$+\alpha_7 RT_{yy} + \alpha_8 RT_{xx} + \alpha_9 \frac{RT}{\rho}\rho_{yy} + \alpha_{10}\frac{RT}{\rho}\rho_{xx}$$
$$+\alpha_{11}\frac{RT}{\rho^2}\rho_y^2 + \alpha_{12}\frac{R}{\rho}T_y\rho_y + \alpha_{13}\frac{R}{T}T_y^2 + \alpha_{14}\frac{RT}{\rho^2}\rho_x^2$$
$$+\alpha_{15}\frac{R}{\rho}T_x\rho_x + \alpha_{16}\frac{R}{T}T_x^2), \tag{10}$$

$$\sigma_{12}^{(2)} = \sigma_{21}^{(2)}$$
$$= \frac{\mu^2}{p}(\beta_1 u_x u_y + \beta_2 u_y v_y + \beta_2 u_x v_x + \beta_1 v_x v_y + \beta_3 RT_{xy}$$
$$+\beta_4 \frac{RT}{\rho}\rho_{xy} + \beta_5 \frac{R}{T}T_x T_y + \beta_6 \frac{RT}{\rho^2}\rho_x\rho_y + \beta_7 \frac{R}{\rho}\rho_x T_y$$
$$+\beta_7 \frac{R}{\rho}T_x\rho_y), \tag{11}$$

$$q_1^{(2)} = \frac{\mu^2}{\rho}(\gamma_1 \frac{1}{T}T_x u_x + \gamma_2 \frac{1}{T}T_x v_y + \gamma_3 u_{xx} + \gamma_4 u_{yy} + \gamma_5 v_{xy}$$
$$+\gamma_6 \frac{1}{T}T_y v_x + \gamma_7 \frac{1}{T}T_y u_y + \gamma_8 \frac{1}{\rho}\rho_x u_x + \gamma_9 \frac{1}{\rho}\rho_x v_y$$
$$+\gamma_{10}\frac{1}{\rho}\rho_y u_y + \gamma_{11}\frac{1}{\rho}\rho_y v_x), \tag{12}$$

and

$$q_2^{(2)} = \frac{\mu^2}{\rho}(\gamma_1 \frac{1}{T}T_y v_y + \gamma_2 \frac{1}{T}T_y u_x + \gamma_3 v_{yy} + \gamma_4 v_{xx} + \gamma_5 u_{xy}$$
$$+\gamma_6 \frac{1}{T}T_x u_y + \gamma_7 \frac{1}{T}T_x v_x + \gamma_8 \frac{1}{\rho}\rho_y v_y + \gamma_9 \frac{1}{\rho}\rho_y u_x$$
$$+\gamma_{10}\frac{1}{\rho}\rho_x v_x + \gamma_{11}\frac{1}{\rho}\rho_x u_y). \tag{13}$$

Both augmented Burnett and BGK-Burnett equations have same forms of the stress tensor and heat flux terms. However the two sets of equations have different values of the coefficients. The coefficients are compared in Table 2.

	Aug. Burnett Eqns. Hard-Sphere gas	BGK-Burnett Eqns. $\gamma = 1.4$	BGK-Burnett Eqns. $\gamma = 1.666$
α_1	1.199	-2.24	-2.222
α_2	0.153	-0.48	-4.444
α_3	-0.600	0.56	1.111
α_4	-0.115	-1.20	-0.667
α_5	1.295	0.0	0.0
α_6	-0.733	0.0	0.0
α_7	0.260	-19.6	-5.833
α_8	-0.130	-5.6	0.0
α_9	-1.352	-1.6	-1.333
α_{10}	0.676	0.4	0.667
α_{11}	1.352	1.6	1.333
α_{12}	-0.898	-19.6	-5.833
α_{13}	0.600	-18.0	-4.5
α_{14}	-0.676	-0.4	-0.667
α_{15}	0.449	-5.6	0.0
α_{16}	-0.300	-6.0	-0.667
β_1	-0.115	-1.4	-1.667
β_2	1.913	-1.4	-1.667
β_3	0.390	0.0	0.0
β_4	-2.028	-2.0	-2.0
β_5	-0.900	2.0	2.0
β_6	2.028	2.0	2.0
β_7	-0.676	0.0	0.0
γ_1	10.830	-25.241	-11.101
γ_2	0.407	-0.2	-1.0
γ_3	-2.269	-1.071	-1.384
γ_4	1.209	-2.0	-2.0
γ_5	-3.478	-2.8	-3.333
γ_6	-0.611	-7.5	-6.5
γ_7	11.033	-11.0	-5.667
γ_8	-2.060	-1.271	-1.051
γ_9	1.030	1.0	1.0
γ_{10}	-1.545	-3.0	-3.0
γ_{11}	-1.545	-3.0	-3.0

Table 2. The coefficients in the Burnett and BGK-Burnett Eqns. stress tensor and heat flux.

The third order approximation (n=3) represents the super Burnett equations. However, not all of the third order terms of the super Burnett equations are used in the augmented Burnett and the BGK-Burnett equations. In the augmented Burnett equations, the third order terms are employed *ad hoc* basis to obtain stable numerical solutions while maintaining second order accuracy of the solutions. The third order terms in the augmented Burnett equations[2] are given as,

$$\sigma_{11}^{(a)} = \frac{\mu^3}{p^2} RT(\alpha_{17} u_{xxx} + \alpha_{17} u_{xyy} + \alpha_{18} v_{xxy} + \alpha_{18} v_{yyy}), \tag{14}$$

$$\sigma_{22}^{(a)} = \frac{\mu^3}{p^2} RT(\alpha_{17} v_{yyy} + \alpha_{17} v_{xxy} + \alpha_{18} u_{xyy} + \alpha_{18} u_{xxx}), \tag{15}$$

$$\sigma_{12}^{(a)} = \sigma_{21}^{(a)} = \frac{\mu^3}{p^2} RT(\beta_8 u_{xxy} + \beta_8 u_{yyy} + \beta_8 v_{xyy} + \beta_8 v_{xxx}), \tag{16}$$

$$q_1^{(a)} = \frac{\mu^3}{p\rho} R(\gamma_{12} T_{xxx} + \gamma_{12} T_{xyy} + \gamma_{13} \frac{T}{\rho} \rho_{xxx} + \gamma_{13} \frac{T}{\rho} \rho_{xyy}), \tag{17}$$

and

$$q_2^{(a)} = \frac{\mu^3}{p\rho} R(\gamma_{12} T_{yyy} + \gamma_{12} T_{xxy} + \gamma_{13} \frac{T}{\rho} \rho_{yyy} + \gamma_{13} \frac{T}{\rho} \rho_{xxy}). \tag{18}$$

The superscript '(a)' denotes augmented Burnett terms. The coefficients in stress and heat flux terms are given in Table 3.

α_{17}	0.2222
α_{18}	-0.1111
β_8	0.1667
γ_{12}	0.6875
γ_{13}	-0.625

Table 3. The coefficients in the augmented Burnett Eqns.

The BGK-Burnett equations have more additional third order terms than the augmented Burnett equations. These are not added on an *ad hoc* basis but are derived from the third order Chapman-Enskog expansion of the BGK-Boltzmann equation. The third order terms in the BGK-Burnett equations[5] are given as

$$\sigma_{11}^{(B)} = \frac{\mu^3}{p^2} RT(\theta_1 u_{xxx} + \theta_2 u_{xyy} + \theta_3 v_{xxy} + \theta_4 v_{yyy}) - \frac{\mu^3}{p^2} \frac{RT}{\rho} (\theta_1 \rho_x u_{xx} + \theta_5 \rho_x v_{xy} + \theta_6 \rho_x u_{yy}$$

$$+\theta_7\rho_y v_{xx}+\theta_8\rho_y u_{xy}+\theta_4\rho_y v_{yy})$$

$$+\frac{\mu^3}{p^2}(\theta_9 u_x^3+3\theta_{10}u_x^2v_y+\theta_{11}u_xv_y^2-\theta_4u_xu_y^2-2\theta_4u_xu_yv_x$$

$$-\theta_4u_xv_x^2+\theta_{10}v_y^3-\theta_{12}v_yu_y^2-2\theta_{12}u_yv_xv_y-\theta_{12}v_x^2v_y)$$

$$+\frac{\mu^3}{p^2}R(\theta_{13}u_xT_{xx}+\theta_{13}u_xT_{yy}+\theta_{14}v_yT_{xx}+\theta_{14}v_yT_{yy}), \tag{19}$$

$$\sigma_{22}^{(B)}=\frac{\mu^3}{p^2}RT(\theta_1v_{yyy}+\theta_2v_{xxy}+\theta_3u_{xyy}+\theta_4u_{xxx})$$

$$-\frac{\mu^3}{p^2}\frac{RT}{\rho}(\theta_1\rho_yv_{yy}+\theta_5\rho_yu_{xy}+\theta_6\rho_yv_{xx}$$

$$+\theta_7\rho_yu_{yy}+\theta_8\rho_xv_{xy}+\theta_4\rho_xu_{xx})$$

$$+\frac{\mu^3}{p^2}(\theta_9v_y^3+3\theta_{10}v_y^2u_x+\theta_{11}v_yu_x^2-\theta_4v_yv_x^2-2\theta_4v_yv_xu_y$$

$$-\theta_4v_yu_y^2+\theta_{10}u_x^3-\theta_{12}u_xv_x^2-2\theta_{12}v_xu_yu_x-\theta_{12}u_y^2u_x)$$

$$+\frac{\mu^3}{p^2}R(\theta_{13}v_yT_{yy}+\theta_{13}v_yT_{xx}+\theta_{14}u_xT_{yy}+\theta_{14}u_xT_{xx}), \tag{20}$$

$$\sigma_{12}^{(B)}=\frac{\mu^3}{p^2}RT(\theta_{15}u_{xxy}+u_{yyy}+\theta_{15}v_{xyy}+v_{xxx})$$

$$-\frac{\mu^3}{p^2}\frac{RT}{\rho}(\theta_6\rho_yu_{xx}+\theta_{16}\rho_yv_{xy}+\rho_yu_{yy}$$

$$+\rho_xv_{xx}+\theta_{16}\rho_xu_{xy}+\theta_6\rho_xv_{yy})$$

$$-\frac{\mu^3}{p^2}(u_y+v_x)(\theta_4u_x^2+2\theta_{12}u_xv_y+2\theta_7u_yv_x$$

$$+\theta_7u_y^2+\theta_7v_x^2+\theta_4v_y^2)$$

$$+\frac{\mu^3}{p^2}R(\theta_{17}u_yT_{xx}+\theta_{17}u_yT_{yy}+\theta_{17}v_xT_{xx}+\theta_{17}v_xT_{yy}), \tag{21}$$

$$q_1^{(B)}=\frac{\mu^3}{p\rho}R(\theta_{18}T_{xxx}+\theta_{18}T_{xyy}-\theta_{18}\frac{1}{\rho}\rho_xT_{xx}-\theta_{18}\frac{1}{\rho}\rho_xT_{yy})$$

$$+\frac{\mu^3}{p\rho}(\theta_{19}u_xu_{xx}+\theta_{20}u_xv_{xy}+\theta_6u_xu_{yy}+\theta_{21}v_yu_{xx}$$

$$+\theta_{22}v_y v_{xy}+\theta_7 v_y u_{yy}+\theta_{23}u_y v_{xx}+\theta_{24}u_y u_{xy}$$
$$+\theta_6 u_y v_{yy}+\theta_{23}v_x v_{xx}+\theta_{24}v_x u_{xy}+\theta_6 v_x v_{yy})$$
$$-\frac{\mu^3}{p\rho}\left(\frac{1}{\rho}\rho_x+\frac{1}{T}T_x\right)(\theta_{13}u_x^2+2\theta_{14}u_x v_y+2\theta_{17}u_y v_x$$
$$+\theta_{17}u_y^2+\theta_{17}v_x^2+\theta_{13}v_y^2)$$
$$+\frac{\mu^3}{p\rho}\frac{R}{T}(\theta_{18}T_x T_{xx}+\theta_{18}T_x T_{yy}), \tag{22}$$

and

$$q_2^{(B)}=\frac{\mu^3}{p\rho}R(\theta_{18}T_{yyy}+\theta_{18}T_{xxy}-\theta_{18}\frac{1}{\rho}\rho_y T_{yy}-\theta_{18}\frac{1}{\rho}\rho_y T_{xx})$$
$$+\frac{\mu^3}{p\rho}(\theta_{19}v_y v_{yy}+\theta_{20}v_y u_{xy}+\theta_6 v_y v_{xx}+\theta_{21}u_x v_{yy}$$
$$+\theta_{22}u_x u_{xy}+\theta_7 u_x v_{xx}+\theta_{23}v_x u_{yy}+\theta_{24}v_x v_{xy}$$
$$+\theta_6 v_x u_{xx}+\theta_{23}u_y u_{yy}+\theta_{24}u_y v_{xy}+\theta_6 u_y u_{xx})$$
$$-\frac{\mu^3}{p\rho}\left(\frac{1}{\rho}\rho_y+\frac{1}{T}T_y\right)(\theta_{13}u_x^2+2\theta_{14}u_x v_y+2\theta_{17}u_y v_x$$
$$+\theta_{17}u_y^2+\theta_{17}v_x^2+\theta_{13}v_y^2)$$
$$+\frac{\mu^3}{p\rho}\frac{R}{T}(\theta_{18}T_y T_{xx}+\theta_{18}T_y T_{yy}). \tag{23}$$

The superscript '(B)' denotes third order stress and heat flux terms in the BGK-Burnett equations. The coefficients of third order terms in the BGK-Burnett equations, θ_i's, are given in Table 4.

	$\gamma = 1.4$	$\gamma = 1.666$
θ_1	2.56	1.778
θ_2	1.36	1.111
θ_3	0.56	-0.222
θ_4	-0.64	-0.889
θ_5	0.96	0.444
θ_6	1.6	1.333
θ_7	-0.4	-0.667
θ_8	-0.24	-0.222
θ_9	1.024	1.185
θ_{10}	-0.256	-0.593
θ_{11}	1.152	1.778
θ_{12}	0.16	0.444

θ_{13}	2.24	2.222
θ_{14}	-0.56	-1.111
θ_{15}	3.6	3.333
θ_{16}	0.6	0.333
θ_{17}	1.4	1.667
θ_{18}	4.9	4.167
θ_{19}	7.04	6.222
θ_{20}	-0.16	-1.778
θ_{21}	-1.76	-3.111
θ_{22}	4.24	4.222
θ_{23}	3.8	4.333
θ_{24}	3.4	3.667

Table 4. The coefficients in the third order terms of BGK-Burnett Eqns.

Finally, the governing equations are nondimensionalized by reference length and free stream variables and coordinate transformed to the computational ξ-η domain by the following relations

$$\tau = t,$$
$$\xi = \xi(x, y),$$

and

$$\eta = \eta(x, y). \tag{24}$$

3. Numerical Method

An explicit finite difference scheme has been employed to solve the governing equations. The Steger-Warming flux-vector splitting method[6] is applied to the inviscid flux terms. The second-order central differencing scheme is applied to the stress tensor and heat flux terms. In the blunt-body flowfield calculations reported in this paper, free stream conditions were used along the outer boundary. First-order extrapolation of the interior data was used to determine the flow properties along the exit boundary. Symmetry boundary conditions were applied to the stagnation streamline. The first-order Maxwell-Smoluchowski slip boundary conditions[2] were used on the wall surface boundary. The first-order Maxwell-Smoluchowski slip boundary conditions in Cartesian coordinates are:

$$u_s = \frac{2-\bar{\sigma}}{\bar{\sigma}} \bar{l} \left(\frac{\partial u}{\partial y} \right)_s + \frac{3}{4} \frac{\mu}{\rho T} \left(\frac{\partial T}{\partial x} \right)_s, \tag{25}$$

and

$$T_s = T_w + \frac{2-\bar{\alpha}}{\bar{\alpha}} \frac{2\gamma}{\gamma+1} \frac{\bar{l}}{\mathrm{Pr}} \left(\frac{\partial T}{\partial y} \right)_s, \tag{26}$$

where

$$\bar{l} = \frac{2\mu}{\rho} \sqrt{\frac{\pi}{8RT}}.$$

The subscript 's' denotes the flow variables on the solid surface of the body. The reflection coefficient, $\bar{\sigma}$, and the accommodation coefficient, $\bar{\alpha}$, were assumed as 1 (for complete accommodation) in this study.

4. Application to Blunt Body

The augmented Burnett and the BGK-Burnett equations are applied to compute the hypersonic flow over a cylindrical leading edge with nose radii of $2m$, $0.2m$, and $0.02\ m$. Since the numbers of grid lines are fixed in ξ and η directions, the smaller cylinder has the finer grid system in the physical domain. The grid system in the physical domain is shown in Fig. 1. The flow conditions are:

$$M_\infty = 10.0$$
$$\mathrm{Re}_\infty = 167.9$$
$$P_\infty = 2.3881\, N/m^2$$
$$T_\infty = 208.4\ ^\circ K$$
$$T_w = 1000.0\ ^\circ K.$$

The coefficient of viscosity is calculated by the Sutherland's law,

$$\mu = c_1 \frac{T^{3/2}}{T + c_2}. \tag{27}$$

Various constants used in the calculation for air are,

$$\gamma = 1.4,$$
$$Pr = 0.72,$$
$$R = 287.04\ m^2/\left(\sec^2 \cdot {}^\circ K\right),$$
$$c_1 = 1.458 \times 10^6\ kg/\sec \cdot m \cdot {}^\circ K^{1/2},$$

and

$$c_2 = 110.4\ ^\circ K.$$

With the given flow conditions and constants, the computations were performed at Knudsen numbers of 0.001, 0.01, and 0.1 corresponding to the cylinder radii of $2m$, $0.2m$, and $0.02m$ respectively.

5. Results and Discussion

5.1. Case 1: ($Kn = 0.1$)

The comparisons of density, velocity, and temperature changes along the stagnation streamline are shown in Figs. 2, 3, and 4 respectively. The results are generally consistent with those of Zhong[2]. The temperature curves (Fig. 4) show that the present augmented Burnett solution using the Steger-Warming scheme has a slightly higher maximum temperature than reported by Zhong[2]. The Navier-Stokes solutions are also compared with the augmented Burnett solutions in Figs. 2 - 4. Since the flow is in the continuum-transition regime in this case, the differences between the Navier-Stokes and the Burnett solutions are significant. The shock width in the augmented Burnett solution is larger and the shock is upstream of that in the Navier-Stokes solution. The density and temperature contours of the Navier-Stokes solutions and the augmented Burnett solutions using the present scheme are shown in Figs. 5 - 8. The shock structure of the present augmented Burnett solutions agrees well with that of Zhong[2]. The BGK-Burnett solutions are currently in progress for this case.

5.2. Case 2: ($Kn = 0.01$)

The comparisons of density, velocity, and temperature changes along the stagnation streamline between the Navier-Stokes, the augmented Burnett, and the BGK-Burnett solutions are shown in Figs. 9, 10, and 11 respectively. The resulting curves are almost coincident with each other. Only small differences are observed at the front of the shock. The velocity curve of the BGK-Burnett solution (Fig. 10) shows an unexpected high peak at the front of the shock. The density and temperature contours of each equation solution are also shown in Figs. 12-17. The shock structures are also similar to each other.

5.3. Case 3: ($Kn = 0.001$)

At this small Knudsen number, the solutions of the Navier-Stokes, the augmented Burnett, and the BGK-Burnett equations are identical. Since the flow is in the continuum regime, the Navier-Stokes equations already describe the flow field accurately. Figs. 18, 19, and 20 show the density, velocity and temperature changes along the stagnation streamline respectively. Figs. 21 - 26 show the density and temperature contours for the Navier-Stokes, the augmented Burnett, and the BGK-Burnett equations.

6. Conclusions

The 2-D augmented Burnett equations and the BGK-Burnett equations have been applied to compute the hypersonic blunt body flow (for air) at Kn = 0.1, 0.01, and 0.001. The explicit finite difference scheme with Steger-Warming flux-vector splitting has been employed to discretize the convective terms in the flow equations. Simple second-order central differencing is used to discretize the stress and heat-flux terms. The density, velocity, and temperature changes along the stagnation streamline were compared for each set of equations. At Kn = 0.1, the resulting flow properties and the shock structure are consistent with the results reported by Zhong[2]. At low Knudsen number ($Kn \leq 0.01$), the Navier-Stokes solutions and the two Burnett solutions are identical. The augmented Burnett equations were always stable at all Knudsen numbers and all grid sizes reported in this paper. However, the BGK-Burnett equations have experienced some convergence problem on the finer grids at Kn=0.1. This issue is being investigated currently.

7. References

1) Fiscko, K.A., and Chapman, D.R., *Comparison of Burnett, Super-Burnett and Monte Carlo Solutions for Hypersonic Shock Structure,* Proceeding of the 16th International Symposium of Rarefied Gas Dynamics, Pasadena, CA, July 1988.

2) Zhong, X., *Development and Computation of Continuum Higher Order Constitutive Relations for High-Altitude Hypersonic Flow,* Ph.D. dissertation, Stanford University, Aug. 1991.

3) Comeaux, K. A., Chapman, D. R., and MacCormack, R. W., *An Analysis of the Burnett Equations Based on the Second Law of Thermodynamics,* AIAA 95-0415, Jan. 1995.

4) Balakrishnan, R., and Agarwal, R. K., *A Kinetic Theory Based Scheme for the Numerical Solution of the BGK-Burnett Equations for Hypersonic Flows in the Continuum Transition Regime,* AIAA Paper 96-0602, Jan. 1996.

5) Balakrishnan, R., and Agarwal, R. K., *Formulation of the 2-D BGK-Burnett Equations,* report (unpublished), Department of Aerospace Engineering, Wichita State University, 1996.

6) Hoffmann, K. A., *Computational Fluid Dynamics for Engineers,* Engineering Education System, Austin, TX , 1989.

Figures

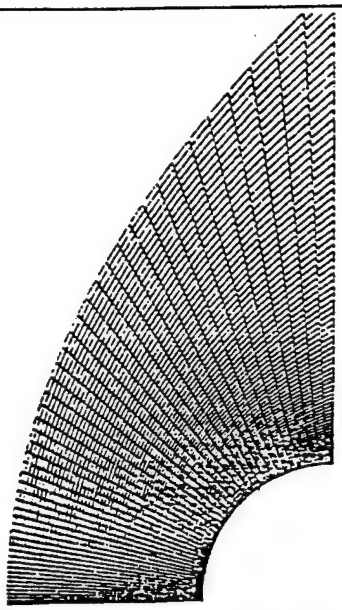

Fig. 1. Computational mesh around a circular cylinder (50×82 grid).

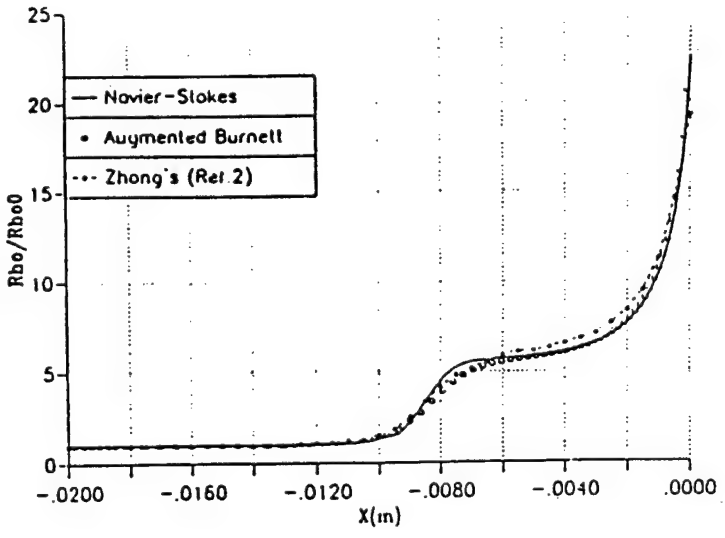

Fig. 2. Density along stagnation streamline for case 1 (Kn=0.1).

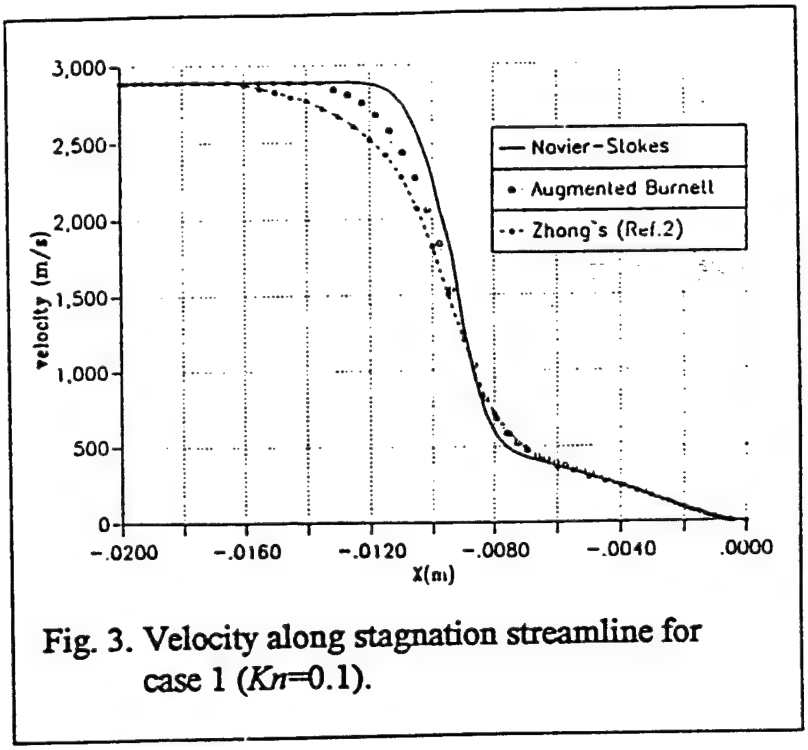

Fig. 3. Velocity along stagnation streamline for case 1 (Kn=0.1).

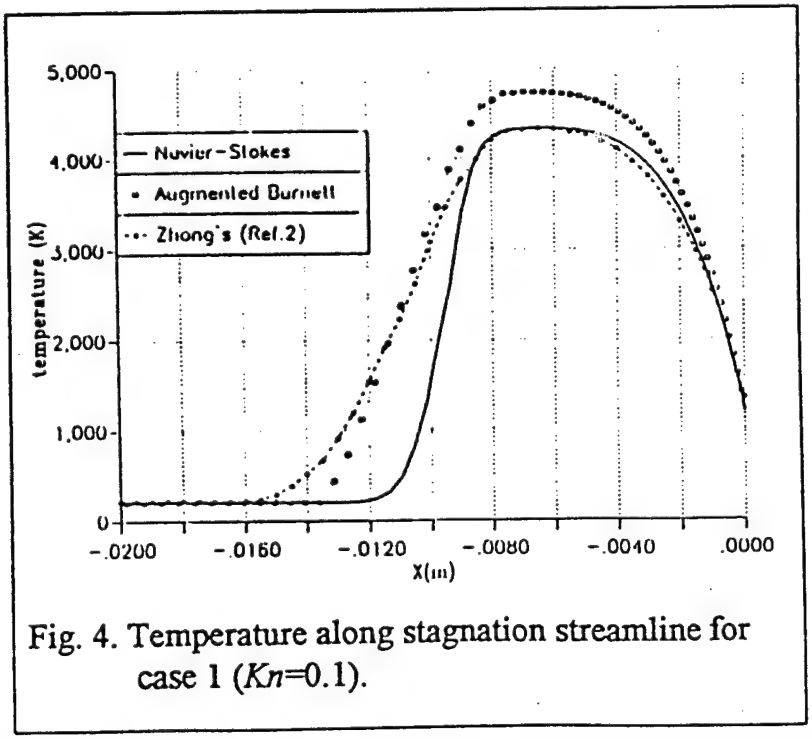

Fig. 4. Temperature along stagnation streamline for case 1 (Kn=0.1).

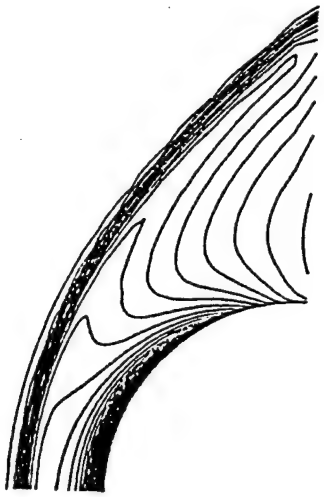

Fig. 5. Navier-Stokes density contours for case 1 (Kn=0.1).

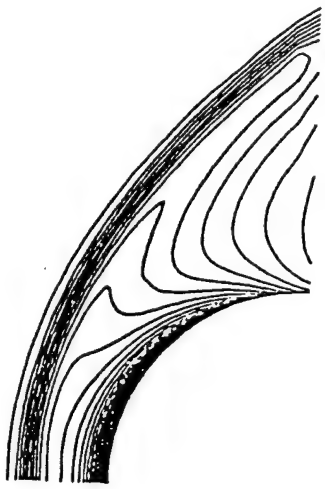

Fig. 6. Augmented Burnett density contours for case 1 (Kn=0.1).

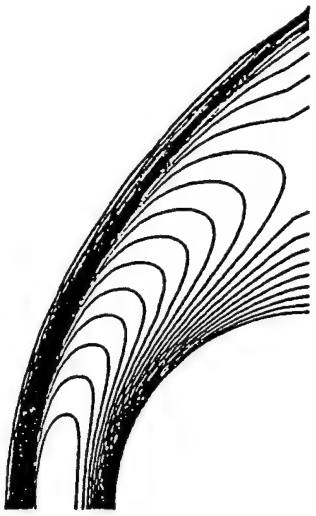

Fig. 7. Navier-Stokes temperature contours for case 1 (Kn=0.1).

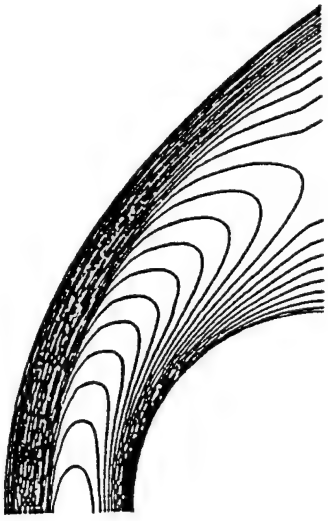

Fig. 8. Augmented Burnett Temperature contours for case 1 (Kn=0.1).

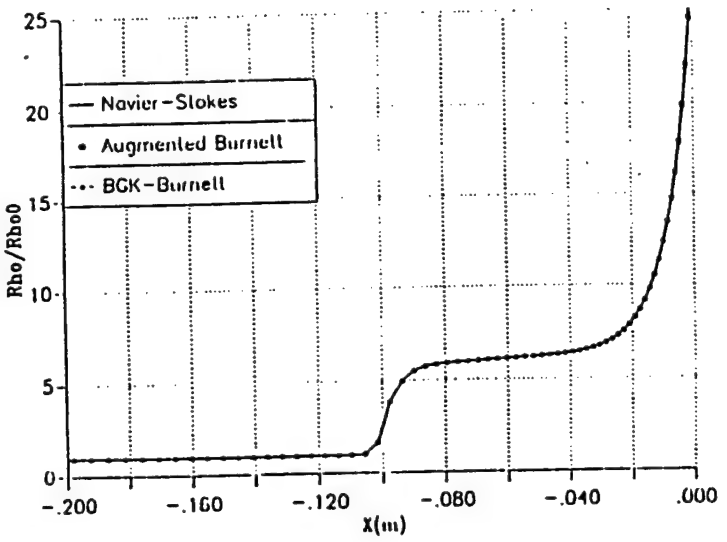

Fig. 9. Density along stagnation streamline for case 2 (Kn=0.01).

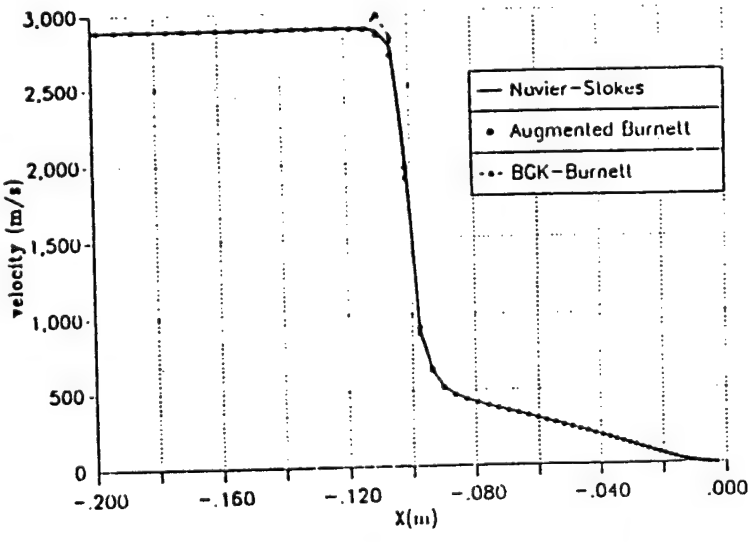

Fig. 10. Velocity along stagnation streamline for case 2 (Kn=0.01).

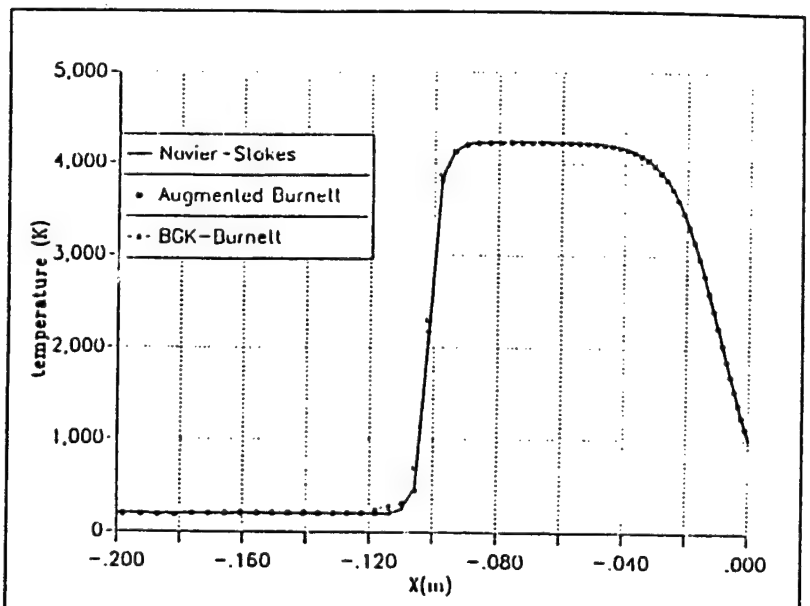

Fig. 11. Temperature along stagnation streamline for case 2 (Kn=0.01).

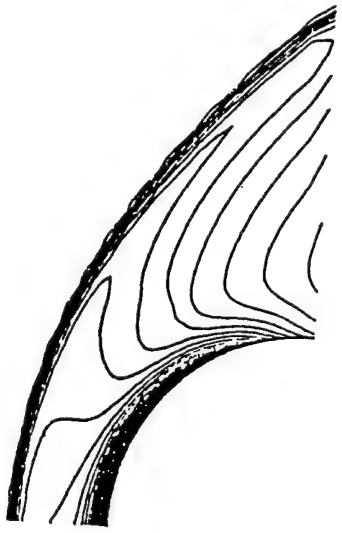

Fig. 12. Navier-Stokes density contours for case 2 (Kn=0.01).

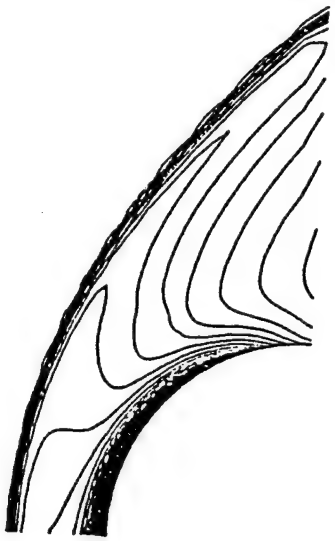

Fig. 13. Augmented Burnett density contours for case 2 (Kn=0.01).

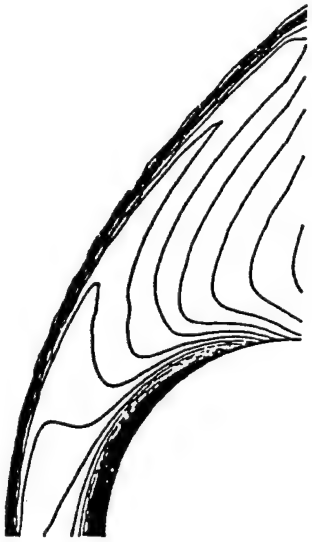

Fig. 14. BGK- Burnett density contours for case 2 (Kn=0.01).

Fig. 15. Navier-Stokes Temperature contours for case 2 (Kn=0.01).

Fig. 16. Augmented Burnett temperature contours for case 2 (Kn=0.01).

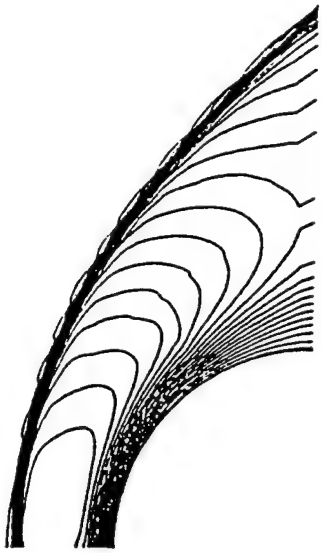

Fig. 17. BGK- Burnett temperature contours for case 2 (Kn=0.01).

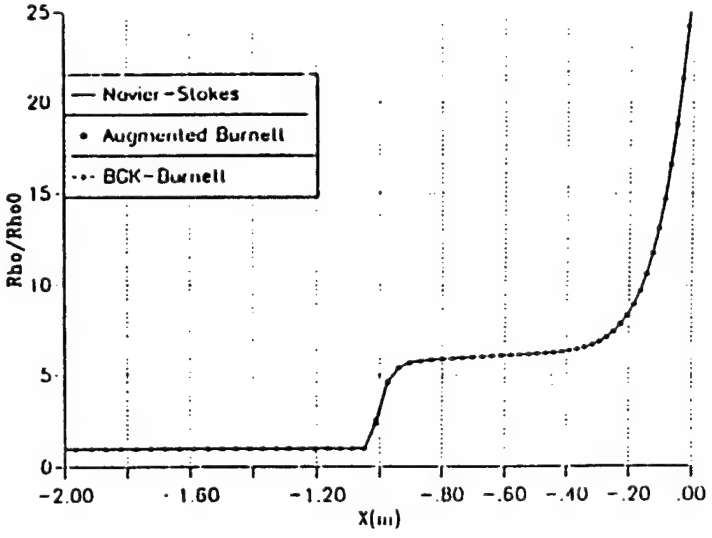

Fig. 18. Density along stagnation streamline for case 3 (Kn=0.001).

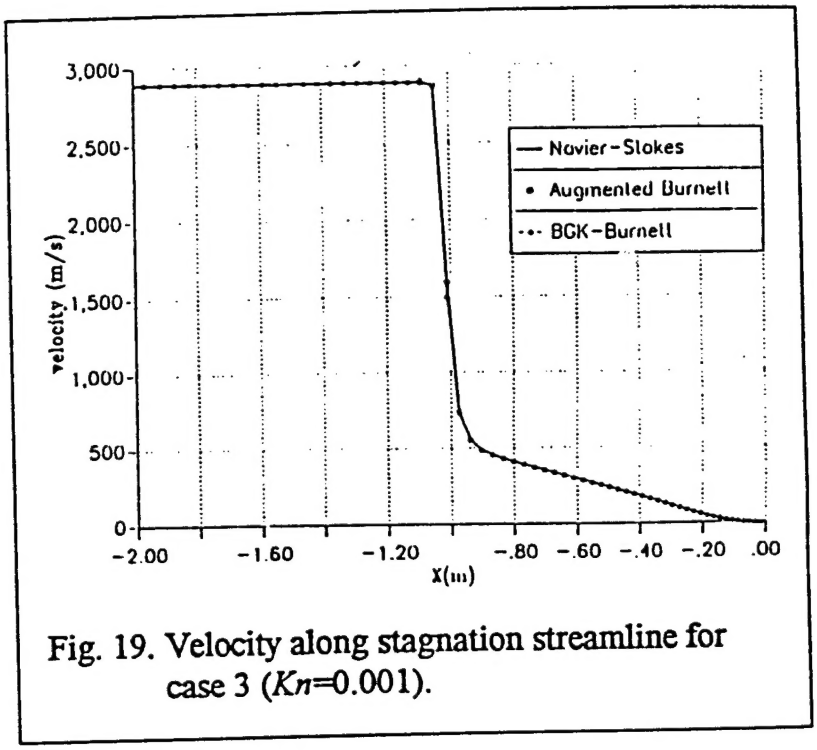

Fig. 19. Velocity along stagnation streamline for case 3 (Kn=0.001).

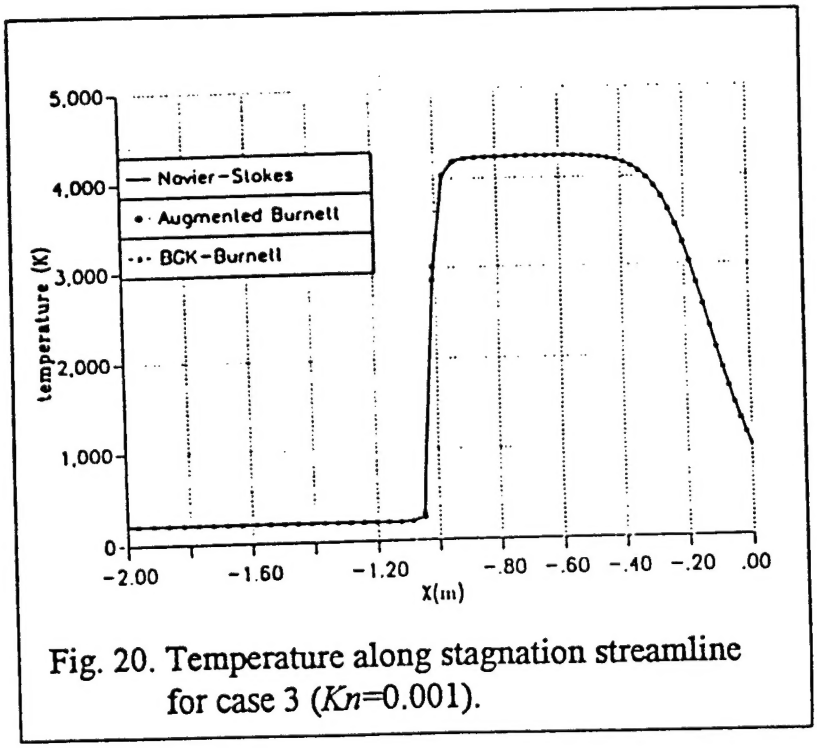

Fig. 20. Temperature along stagnation streamline for case 3 (Kn=0.001).

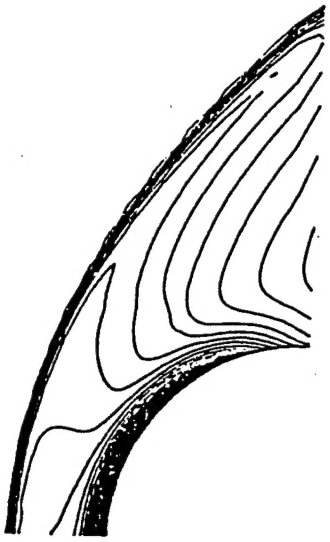

Fig. 21. Navier-Stokes density contours for case 3 (Kn=0.001).

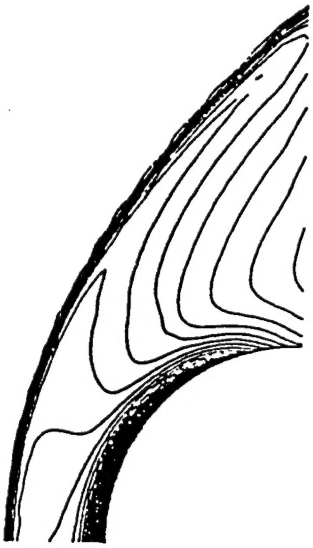

Fig. 22. Augmented Burnett density contours for case 3 (Kn=0.001).

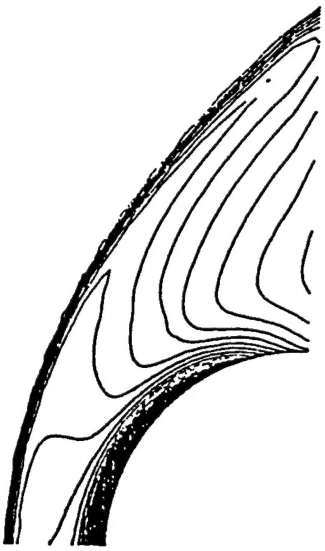

Fig. 23. BGK-Burnett density contours for case 3 (Kn=0.001).

Fig. 24. Navier-Stokes Temperature contours for case 3 (Kn=0.001).

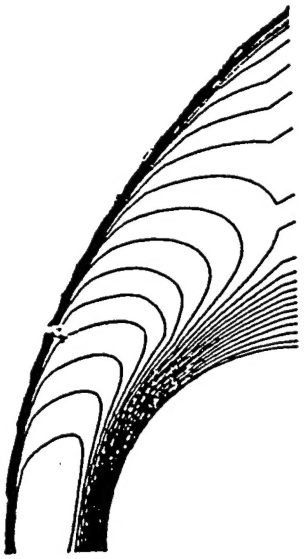

Fig. 25. Augmented Burnett Temperature contours for case 3 (Kn=0.001).

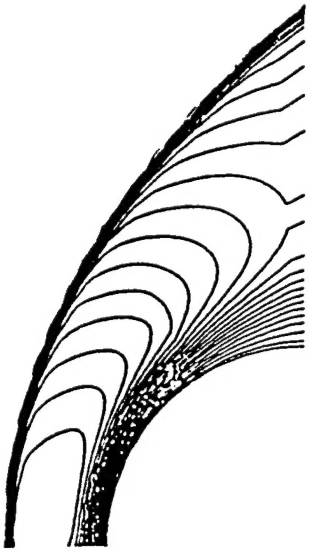

Fig. 26. BGK-Burnett Temperature contours for case 3 (Kn=0.001).